UCRL-13923

REPORT NO. CASD-LLL-78-007
CONTRACT 9815603

CONFIRMATORY ANALYSIS & DETAIL DESIGN OF THE MAGNET SYSTEM FOR MIRROR FUSION TEST FACILITY (MFTF)

EXECUTIVE SUMMARY

GENERAL DYNAMICS
Convair Division

REPORT NO CASD-LLL-78-007

CONFIRMATORY ANALYSIS & DETAIL DESIGN OF THE MAGNET SYSTEM FOR MIRROR FUSION TEST FACILITY (MFTF)

EXECUTIVE SUMMARY

October 1978

R.E. Tatro
R.W. Baldi

Prepared Under
Contract 9815603

Prepared for
UNIVERSITY OF CALIFORNIA
LAWRENCE LIVERMORE LABORATORY
P.O. Box 5012 (L-446)
Livermore, California 94550

Prepared by
GENERAL DYNAMICS CONVAIR DIVISION
P.O. Box 80847
San Diego, California 92138

THIS DOCUMENT PREPARED BY
GENERAL DYNAMICS/CONVAIR
AND APPROVED BY

R. W. BALDI
CHIEF ENGINEER
MFTF MAGNET SYSTEM

R. E. TATRO
PROGRAM MANAGER
MFTF MAGNET SYSTEM

TABLE OF CONTENTS

LIST OF FIGURES

LIST OF FIGURES, Contd

LIST OF TABLES

SUMMARY

The basic objectives of the program were to perform confirmatory analyses of the Lawrence Livermore Laboratory (LLL) Mirror Fusion Test Facility (MFTF) magnet system conceptual design, and then to complete the detailed design of the entire magnet system. Producibility was a major consideration in our selection of materials, processes and detail design features.

General Dynamics has sought to maintain the proper balance between engineering excellence and LLL schedule and cost constraints, remembering that an adequate design is often best. We sought to develop a thorough understanding of the functions and interactions between the various magnet systems, and between the magnet and other MFTF systems such as the vacuum vessel and the NBIS. We sought to develop open harmoneous working relationships between the LLL and General Dynamics MFTF staffs.

We believe we have achieved all of these objectives within the challenging program schedule and within the budgeted funds. We have received the full cooperation of the LLL MFTF program staff and have participated with them as a full partner in identifying problems, and in suggesting, evaluating, and selecting solutions. We have delivered to LLL six discrete reports:

Literature Survey (Helium Heat Transfer)	CASD-LLL-78-001
Thermodynamic Analysis	CASD-LLL-78-002
Structural Analysis	CASD-LLL-78-003
Manufacturing/Producibility Study	CASD-LLL-78-004
Instrumentation Plan	CASD-LLL-78-005
Quality Assurance Report	CASD-LLL-78-006

We have also delivered 75 drawings (125 sheets) with which LLL can procure and fabricate the magnet system.

We conclude this program with a high degree of confidence that the Lawrence Livermore Laboratory Mirror Fusion Test Facility magnet system design will satisfy the program objectives, and that it can be economically fabricated.

1

THERMODYNAMICS

We have completed a literature survey on helium heat transfer and a series of detailed analyses to support design of the MFTF magnet system, including thermal analyses of magnet cooldown and warmup, and design analyses of the magnet thermal shield systems and structural supports. We have also performed a cryostability analysis of the MFTF magnet conductor. We have investigated the problem of emergency shutdown analysis with respect to possible employment of our thermal analysis models. The literature survey is presented in CASD-LLL-78-001, "A Literature Survey of Helium Heat Transfer to Support Magnet System Thermal Control Design for Mirror Fusion Test Facility (MFTF)." Documentation of the thermal analyses is contained in CASD-LLL-78-002, "Thermodynamic Analysis of the Magnet System For Mirror Fusion Test Facility (MFTF)."

1.1 LITERATURE SEARCH

CASD-LLL-78-001 presents summaries of pertinent literature in the field of helium heat transfer with particular emphasis on the applicability to cooldown/warmup and cryostability of superconducting magnets. The task was initiated with a request to NBS Boulder for a computerized literature search on subject areas: liquid helium heat transfer, gas helium heat transfer, and cooling superconducting magnets. This resulted in a listing of 1500 articles covering the period 1956 to 1978; however most of the studies were conducted within the last ten years. The initial listing was scanned for pertinent keywords or titles and was reduced to approximately 150 articles. These articles were cited and the 28 most pertinent to our current study were selected for summarizing. The results of this task provide recommended correlations for design analysis of heat transfer on flat surfaces or in narrow channels for various orientations.

1.2 COOLDOWN/WARMUP

Our cooldown and warmup thermal analyses included investigation of a broad range of flow rates and supply temperature schedules. We have achieved all analysis objectives, including definition of a range of cooldown and warmup operating schedules which (1) can effect complete cooldown within three to five days (a LLL requirement), (2) yield acceptable levels of thermally-induced stresses resulting from transverse and longitudinal structural temperature differentials, and (3) yield acceptable stress levels due to dissimilar flow rates (flow imbalances) in separate sections of the magnet.

Our cooldown and warmup studies were initiated with the formulation of a detailed, multinode analysis model of the magnet in its initial orientation, with vertical

alignment of the z-axis. The quarter-symmetrical model of a single yin or yang permitted thermal simulation of any section of the total assembly by simple re-direction of the helium through-flow nodal arrangement. The analysis model contained 738 nodes, and conveniently exploited thermal symmetry, in that helium entry and exit locations were always at the major and/or minor radii of each magnet.

Reorientation of the magnet assembly necessitated redesign of our analysis model which we presented at the Preliminary Design Review (PDR) on 10 July 1978. The revised analysis model consisted of two sections containing 629 nodes and 1280 nodes, respectively. It also contained simulations of the external case stiffeners and the intercoil structure, and realistically modeled the structural thermal asymmetry resulting from repositioning of the helium entry and exit locations to the lowest and highest points on each magnet.

Later case stiffener modifications were incorporated in the final configuration of our cooldown and warmup analysis model. The model was also reduced in size, to the arrangement shown in Figure 1. In this arrangement, the regions identified as "Large Model 1" and "Large Model 2" comprised the 1280-node section of the PDR analysis model. This change permitted more economical execution of the analyses on the National Magnet Fusion Energy Computer Center (NMFECC). Large Models 1 and 2, shown in Figure 1, were then employed to assess the transverse temperature gradients in the magnet structure. In order to provide temperature boundary conditions for the large analysis models, and to permit multiple analyses yielding total system cooldown time, the exacting multi-node simulations in each section of the large model (see Figure 1) were condensed and assembled into a 44-node small model of an entire magnet. The small model, shown in Figure 2, was then employed in a series of cooldown analyses with flow rates ranging 51 G/sec to 340 G/sec.

Transverse temperature differentials, developed with the large model, were found to yield acceptable stress levels for flow rates approaching 180 G/sec, with a total cooldown time of only 30 hours. Longitudinal temperature differentials, obtained with the small model, proved to establish the limiting thermal stress levels. For analysis purposes, a cooldown helium supply temperature schedule was selected having successive 18-hour intervals with supply temperatures of 225K, 150K, 75K, and 4.5K, respectively. These studies yielded total magnet cooldown times of 72.4 hours for a flow rate of 119 G/sec, 80.8 hours for 102 G/sec, and 90.8 hours for 85 G/sec. Temperature distributions corresponding to the 119 G/sec flowrate and the 85 G/sec flowrate were imposed on separate legs of a single magnet, yielding acceptable stress levels. We therefore recommend a nominal total flowrate of 100 G/sec, and predict a cooldown period of 82 ± 10 hours.

1.3 CRYOSTABILITY ANALYSIS

We have completed a cryostability analysis of the MFTF conductor, using the NMFECC, and employing the thermal analysis computer model shown in Figure 3. In order to gain

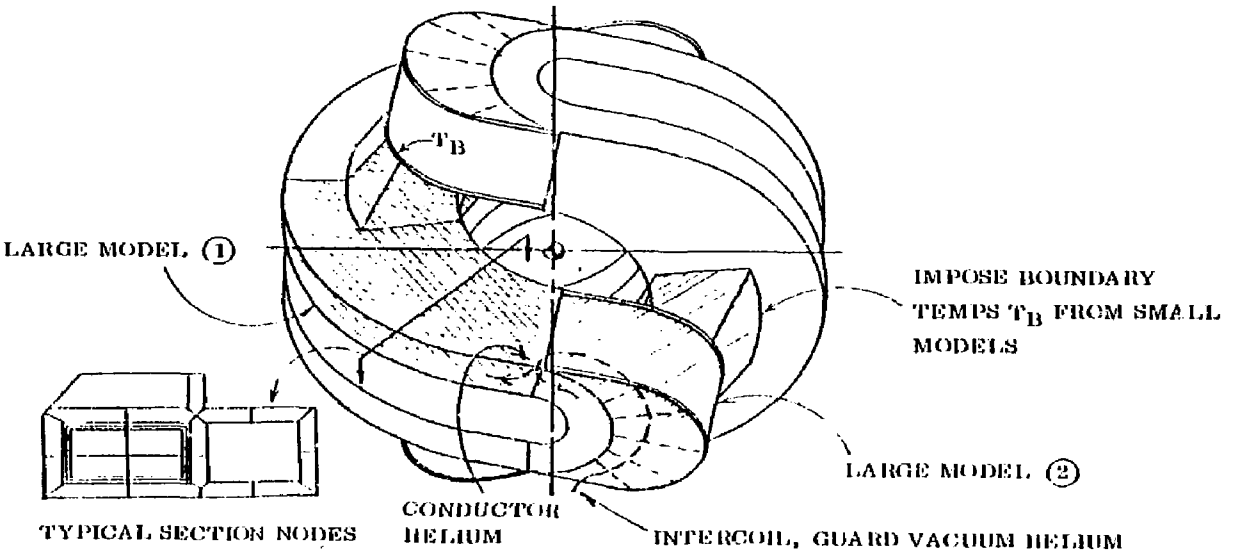

Figure 1. Final Configuration, Cooldown/Warmup Thermal Analysis Large Models

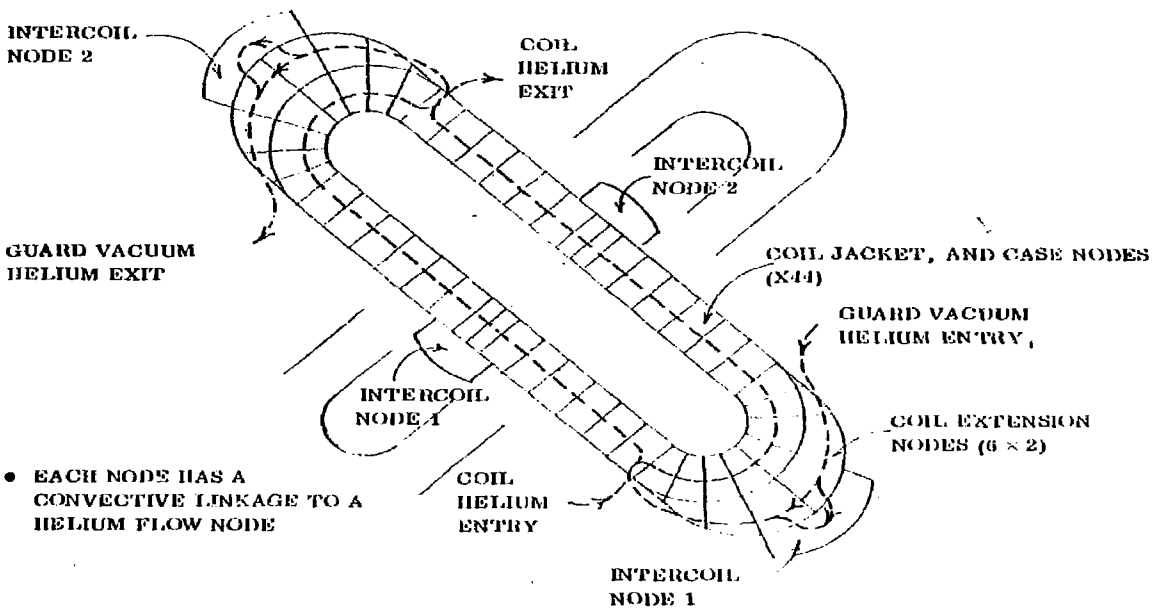

Figure 2. Cooldown/Warmup Thermal Analysis Small Model Configuration

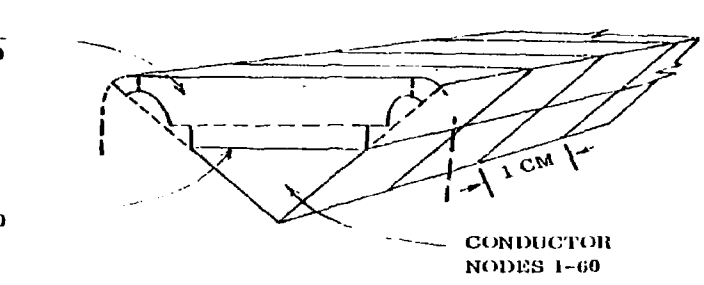

CONDUCTOR NODES, 1-60

- MASS = 0.6874g
- AREA TO HELIUM = 0.3289 cm^2

STABILIZER NODES, 201-260

- MASS = 1.7975g
- AREA TO HELIUM = 1.7175 cm^2

INTERNODAL CONDUCTIVE RESISTANCE

$$R_{1-2} = \frac{547.07}{k_{sc}} \text{ K/W}, \quad R_{201-202} = \frac{261.145}{k_{cu}} \text{ K/W}, \quad R_{1-101} = \frac{12.753}{k_{sc}} \text{ K/W}, \quad R_{101-201} \quad \frac{30.57}{k_{cu}} \text{ K/W}$$

CONDUCTOR: RRR = 150, ρ_{11-0} @ 4.5K = $0.01216 \times 10^{-8}\ \Omega$M

STABILIZER: RRR = 220, ρ_{11-0} @ 4.5K = $0.00829 \times 10^{-8}\ \Omega$M

KOHLER PLOT EMPLOYED FOR MAGNETO-RESISTIVITY

THERMAL CONDUCTIVITY BASED ON WIEDEMANN-FRANZ LAW

Figure 3. MFTF Magnet Conductor Cryostability Analysis Thermal Model

a complete assessment of the conductor recovery characteristics, we analyzed the following conditions: (1) 7.68 Tesla (5775 amps), the current maximum design magnetic field, (2) 7.775 Tesla (5846 amps), the maximum field for which recovery is unconditional, (3) 7.83 Tesla (5883 amps), in which recovery is by cold-end condition, (4) 7.885 Tesla (5929 amps) which approaches a non-recovery condition, (5) 7.95 Tesla (5978 amps), in which a stable boiling non-recovery occurs, and (6) 7.68 Tesla with simulation of a worst-case solder flaw condition. The initial fault condition was simulated by imposition of a 30K temperature over 40 cm of the 60-cm analysis model, per LLL recommendation, an energy deposition of 2.085 J/cm^3. The analysis data compares favorably with LLL one-meter bore preliminary test data, confirming a non-recovery ohmic heating of 1.637 W/cm.

1.4 THERMAL SHIELD ANALYSIS

We have also performed detailed thermal design analyses of the neutral beam impingement H_2O shield, the plasma H_2O shield, the LN_2 magnet shield, all shield support brackets, and the hanger and stabilizer rods. Resulting thermal response characteristics verify the soundness of the thermal control designs. Our final estimate of total refrigeration heat load is 238.2 W plus 32.2 ℓ/hr for the LHe system.

1.5 EMERGENCY SHUTDOWN PROCEDURE

An evaluation was made of our cooldown/warmup and cryostability analysis models as potential analysis tools for studies of emergency shutdown conditions. Our cooldown analysis model is designed to assess temperature excursions in the massive magnet structure. Because emergency shutdown phenomena are of relatively brief duration (i.e., 60 seconds), we have concluded that our cooldown and warmup analysis models would not be useful to an analysis of emergency shutdown conditions. Our cryostability analysis model could have limited application in estimating quench propagation velocities. However, another exiting Convair quench pressure model is available and with modifications it can be applied to the analysis of MFTF emergency shutdown conditions.

2

STRUCTURAL ANALYSIS

We have performed a detailed stress analysis that has confirmed the structural integrity of the MFTF magnet case, jacket and shield system. This analysis is documented in Report No. CASD-LLL-78-003. Key structural criteria were defined by LLL and included the requirement for a 1.5 factor of safety on yield strength, material definition and allowables, and design loading conditions. Finite element analysis methods were used to determine stresses in the case jacket, and support structure for thermal, pressure, inertia (seismic and handling), and magnetic loads. Figure 4 illustrates the large, 5000 degree of freedom GDSAP model used to determine stresses and deflections due to electro-magnetic forces, quench pressure, and 4.5K operation. Interactive computer graphics shown in Figure 5 were used to confirm input data for the model and to display deflected structural shapes calculated by the finite element analyses. These techniques are required to validate a finite element analysis model of this size .

The MFTF finite element model accurately represents the case and jacket structure and simulates the conductor pack stiffness with an array of interconnected rod elements. The model determines the interaction between the structure and conductor pack due to the 22 million pounds of magnetic force, and due to differential thermal contraction. Standard analysis methods were used to analyze magnet support system detailed parts, the thermal shields, and their supports.

The LLL conceptual design which was used as a baseline for our structural analysis had an unstiffened case made of 21-6-9 stainless steel with inconel 625 welds. The intercoil structure was undefined, and was represented in our original finite element analysis by a simple beam element. The initial finite element analysis of the magnet case revealed excessive secondary bending stresses in the corners of the outer case plate caused by magnetic pressures and excessive tension stresses in the inner case plate of the minor radius. Our preliminary fracture analysis of the 21-6-9 plate and inconel 625 weld metal was based on assumed properties for 3 inch thick plate. It predicted an allowable operating stress of 75 KSI which was less than the allowable stress based on yield strength divided by 1.5. The stress and fracture analysis data were presented to LLL on 2 June 1978 along with recommended solutions to the high stress problems.

After the 2 June 1978 presentation, our analyses investigated the effect of case stiffeners on the highly stressed side plate, and we incorporate the intercoil structure into our finite element analysis model. At the same time, several LLL-directed changes were incorporated into our analysis, and we performed a fracture analysis of 304LN material in support of a possible case material change. The LLL-directed changes included displacing the magnets by 10 cm each (a total of 20 cm), and the definition of neutral beam

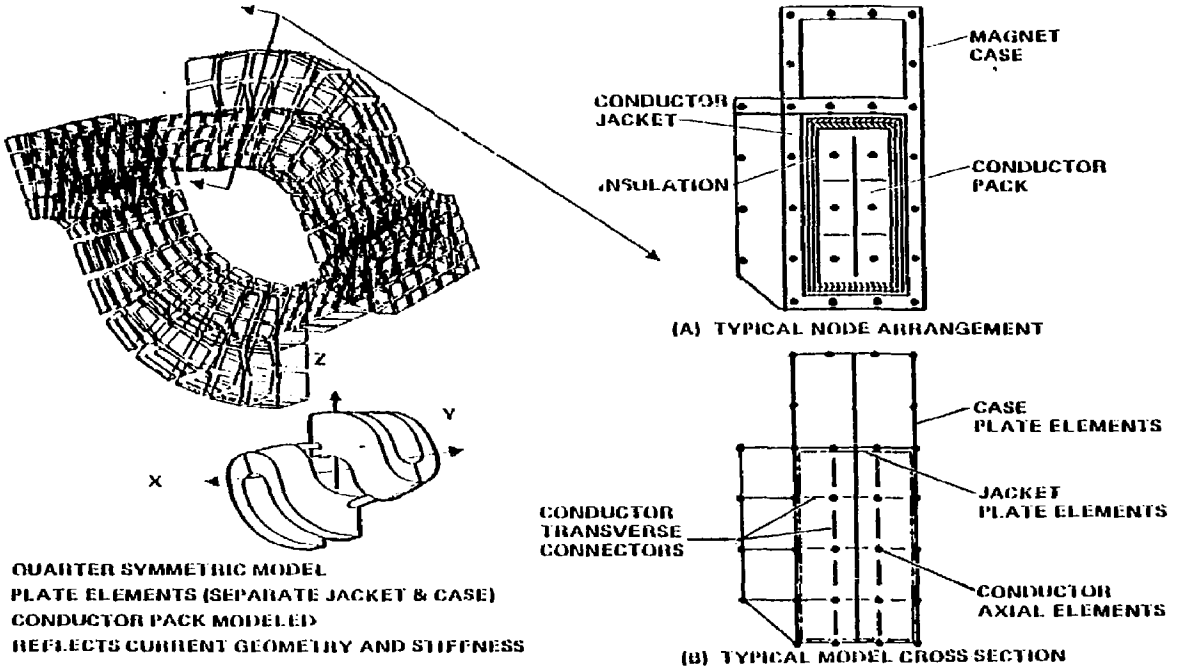

Figure 4. MFTF GDSAP Finite Element Model

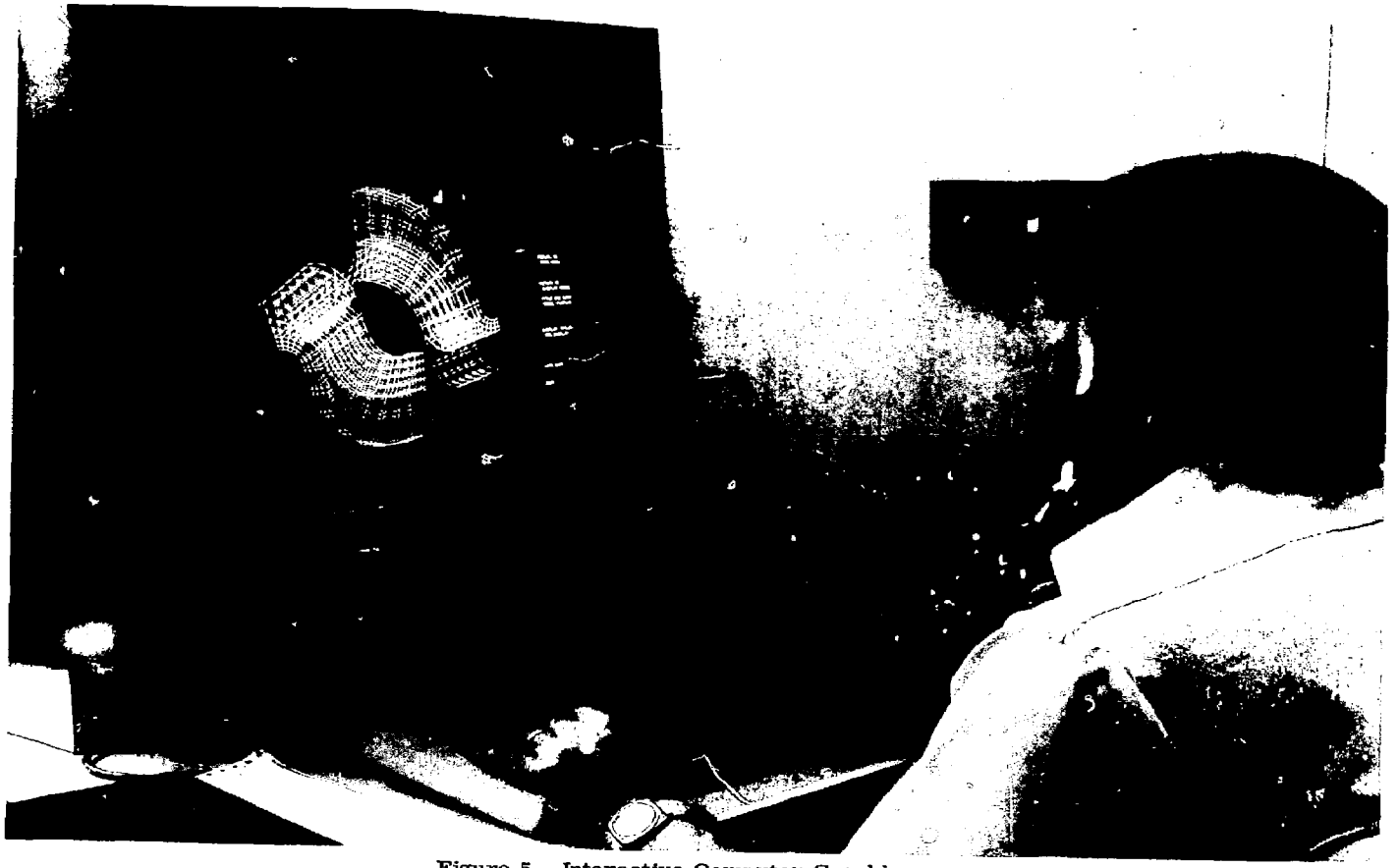

Figure 5. Interactive Computer Graphics

and diagnostic access requirements that necessitated chamfering the magnet case in critical areas. Displacing the magnets resulted in an increase in magnetic loads of 10 to 20 percent. Our analysis of the resulting configuration showed that the secondary bending problem on the case plates was essentially solved but that the other changes had increased the peak minor radius tension stress to 105 KSI. This data was presented at the PDR on 10 July 1978, where several potential changes were recommended to solve the minor radius stress problem.

Stress analysis immediately after PDR confirmed that significant changes were required to reduce the stresses in the minor radius to an acceptable level. The LLL directed change to 304LN case material resulted in an allowable operating stress of 80 KSI based on an anticipated yield strength of 120 KSI. In order to reduce the peak minor radius stresses to 80 KSI, it was necessary to increase the depth of the magnet case by 15%, increase the inner case plate from 2 to 3 inches, and increase two of the case crossover plates in the minor radius from 3 to 5 inches. These changes, combined with the extension of the center crossover plate, resulted in a case configuration where all of the peak stresses have the required 1.5 factor of safety on the yield strength. Fracture analysis of the 304LN plate and 316L weld metal predicts that up to this stress level, the MFTF magnet can satisfactorily sustain the anticipated 500 charge/discharge cycles. Peak principal stresses calculated by the finite element analysis are shown in Figure 6.

A small beam element analysis model of the complete magnet system and its support struts was created after PDR to calculate overall magnet loads due to cooldown thermal gradients and seismic load factors. The unsymmetric cooldown temperature distributions caused by the change to a horizontal fusion chamber, and the redundancy of the support system necessitated the creation of this analysis model. The model determined that the projected cooldown stresses were well within the allowable case stresses. Support strut loads based on 1-g vertical and 0.75-g lateral magnet seismic accelerations were also found to be within the capability of the supports which had been designed for hand calculated seismic and handling loads. However, the model revealed that high loads were developed in the support struts due to the thermal contractions of the struts. When these loads were added to the seismic loads, the design capability of one of the hanger support struts was exceeded. We recommended that the support system could be redesigned in coordination with the fusion chamber to reduce or eliminate the support redundancy.

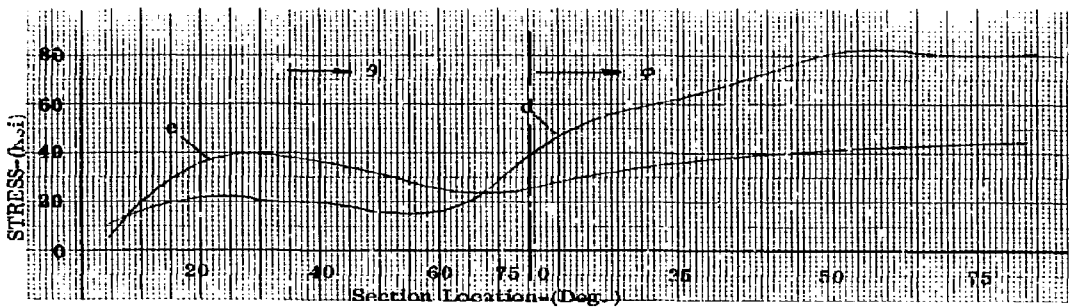

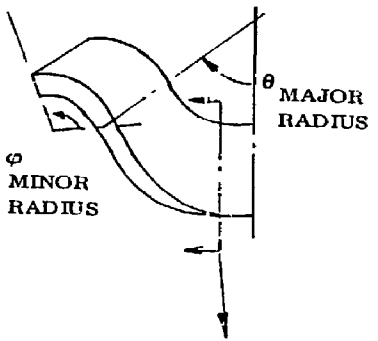

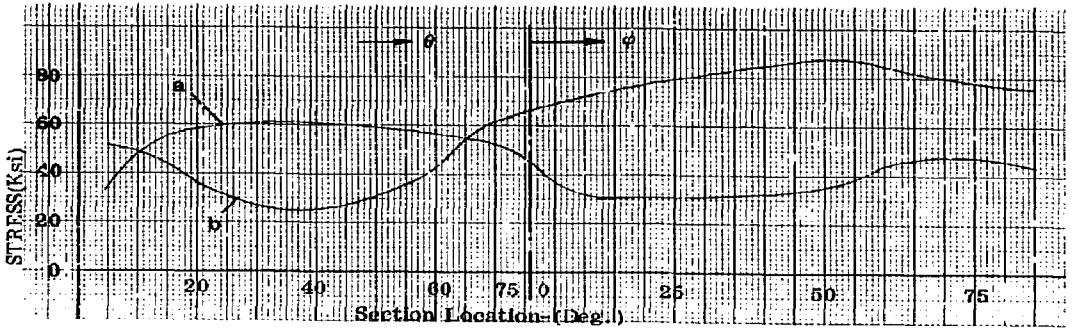

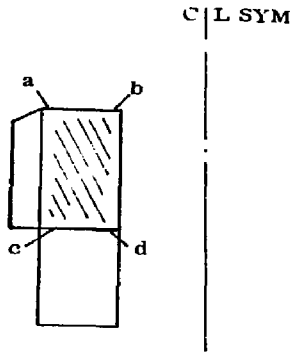

Figure 6. Magnet Case Principal Stresses

3

DESIGN

The design of the magnet system incorporates the three basic areas of jacket design, case design, and support and penetration design. The preparation of 75 drawings was required to complete the design, many of which consist of multiple sheets. The drawing tree, Figure 7, shows the drawings and their assembly into the top drawing which is the magnet installation. Computer Aided Design drafting equipment was utilized in preparing some of the magnet case drawings as shown in Figure 8 & 9.

3.1 JACKET DESIGN

The design of the jacket embodies features that provide for:

- Electrical insulation of the conductor bundle.
- Clamping of the conductor bundle to restrain conductor keystoning.
- Helium plenum within the jacket enclosure.
- Support of conductor leads entering the jacket.
- Shimming to transmit coil magnetic forces to the jacket.
- Jacket assembly that fits tight to the shimmed conductor bundle.
- Jacket close out welds that do not damage the enclosed coil elements.

Electrical insulation of the conductor bundle is accomplished by surrounding the conductor bundle with five layers of 5 mil Kapton. The joints in each layer are overlapped by the succeeding layer so as to provide a dielectric breakdown creepage helium path of at least 2 inches. The use of the Kapton at the conductor bundle corners as shown in Figure 10, is particularly advantageous, since it does not interfere with the winding operation, and can be subsequently folded into place after the winding is complete.

Integral coil clamps are provided to replace the winding fixture clamps used during winding. Four adjustable bars, located at the small radius, are forced and retained against the upper surface of the conductor bundle. Restraining the conductors at the small radius ends also restrains the conductors throughout the bundle. The coil clamps remain within the jacket during jacket assembly.

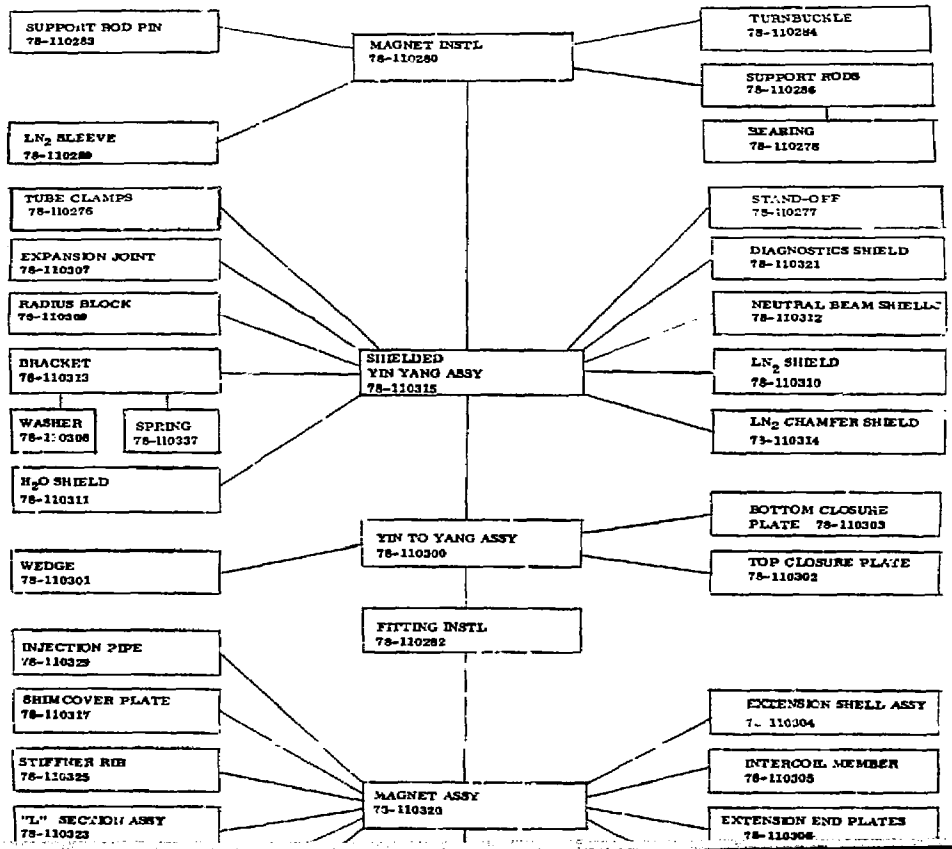
SUPPORT ROD PIN
78-110283
MAGNET INSTL
78-110280
TURNBUCKLE
78-110284
SUPPORT RODS
78-110286
LN_2 SLEEVE
78-110289
BEARING
78-110276
TUBE CLAMPS
78-110276
STAND-OFF
78-110277
EXPANSION JOINT
78-110307
DIAGNOSTICS SHIELD
78-110321
RADIUS BLOCK
78-110309
NEUTRAL BEAM SHIELD
78-110312
BRACKET
78-110313
SHIELDED
YIN YANG ASSY
78-110315
LN_2 SHIELD
78-110310
WASHER
78-110308
SPRING
78-110337
LN_2 CHAMFER SHIELD
78-110314
H_2O SHIELD
78-110311
BOTTOM CLOSURE
PLATE 78-110303
YIN TO YANG ASSY
78-110300
WEDGE
78-110301
TOP CLOSURE PLATE
78-110302
FITTING INSTL
78-110282
INJECTION PIPE
78-110329
SHIMCOVER PLATE
78-110317
EXTENSION SHELL ASSY
78-110304
STIFFNER RIB
78-110325
INTERCOIL MEMBER
78-110305
MAGNET ASSY
78-110320
"L" SECTION ASSY
78-110323
EXTENSION END PLATES
78-110306

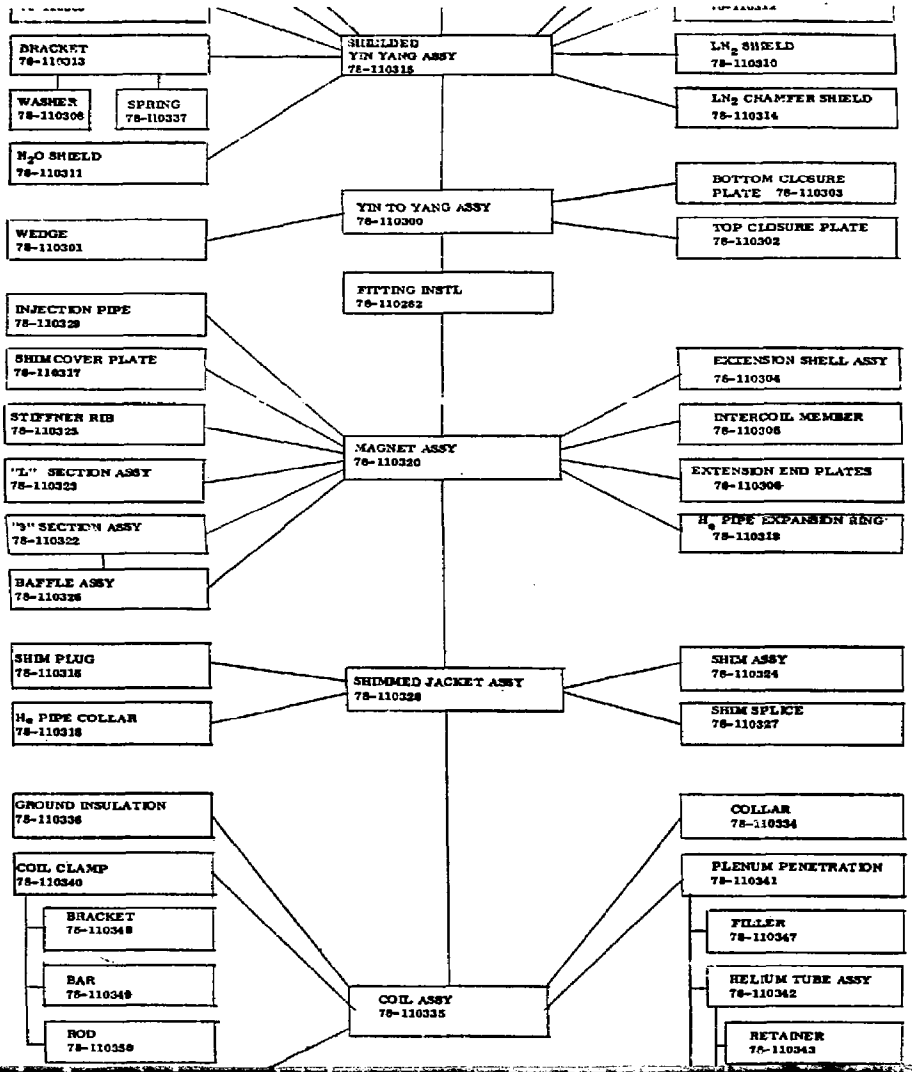
BRACKET
78-110313
WASHER
78-110306
SPRING
78-110337
H_2O SHIELD
78-110311
SHIELDED
YIN YANG ASSY
78-110315
LN_2 SHIELD
78-110310
LN_2 CHAMFER SHIELD
78-110314
BOTTOM CLOSURE
PLATE 78-110303
YIN TO YANG ASSY
78-110300
WEDGE
78-110301
TOP CLOSURE PLATE
78-110302
FITTING INSTL
78-110282
INJECTION PIPE
78-110329
SHIM COVER PLATE
78-110317
STIFFNER RIB
78-110325
"L" SECTION ASSY
78-110323
"S" SECTION ASSY
78-110322
BAFFLE ASSY
78-110326
EXCENSION SHELL ASSY
78-110304
INTERCOIL MEMBER
78-110305
MAGNET ASSY
78-110320
EXTENSION END PLATES
78-110306
H_e PIPE EXPANSION RING
78-110319
SHIM PLUG
78-110318
H_e PIPE COLLAR
78-110316
SHIMMED JACKET ASSY
78-110328
SHIM ASSY
78-110324
SHIM SPLICE
78-110327
GROUND INSULATION
78-110336
COIL CLAMP
78-110340
BRACKET
78-110348
BAR
78-110349
ROD
78-110350
COIL ASSY
78-110335
COLLAR
78-110334
PLENUM PENETRATION
78-110341
FILLER
78-110347
HELIUM TUBE ASSY
78-110342
RETAINER
78-110343

Figure

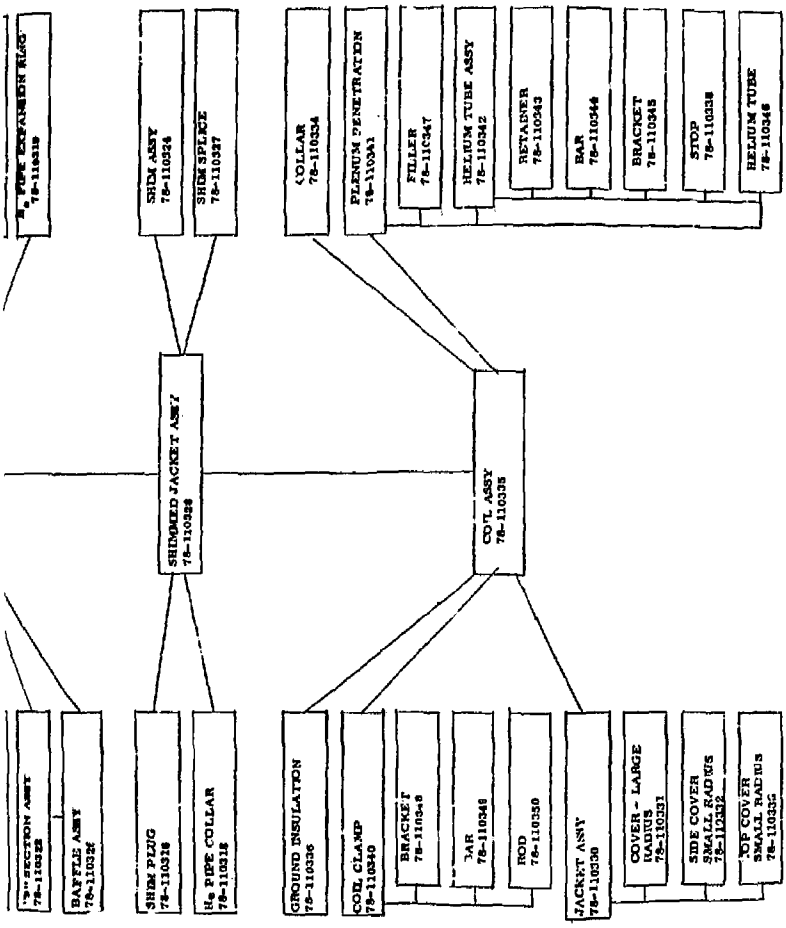

Figure 7. MFTF Magnet System Drawing Tree

Figure 8. Preliminary Designs Were Reviewed on Computer Aided Design (CAD) Interactive Graphics

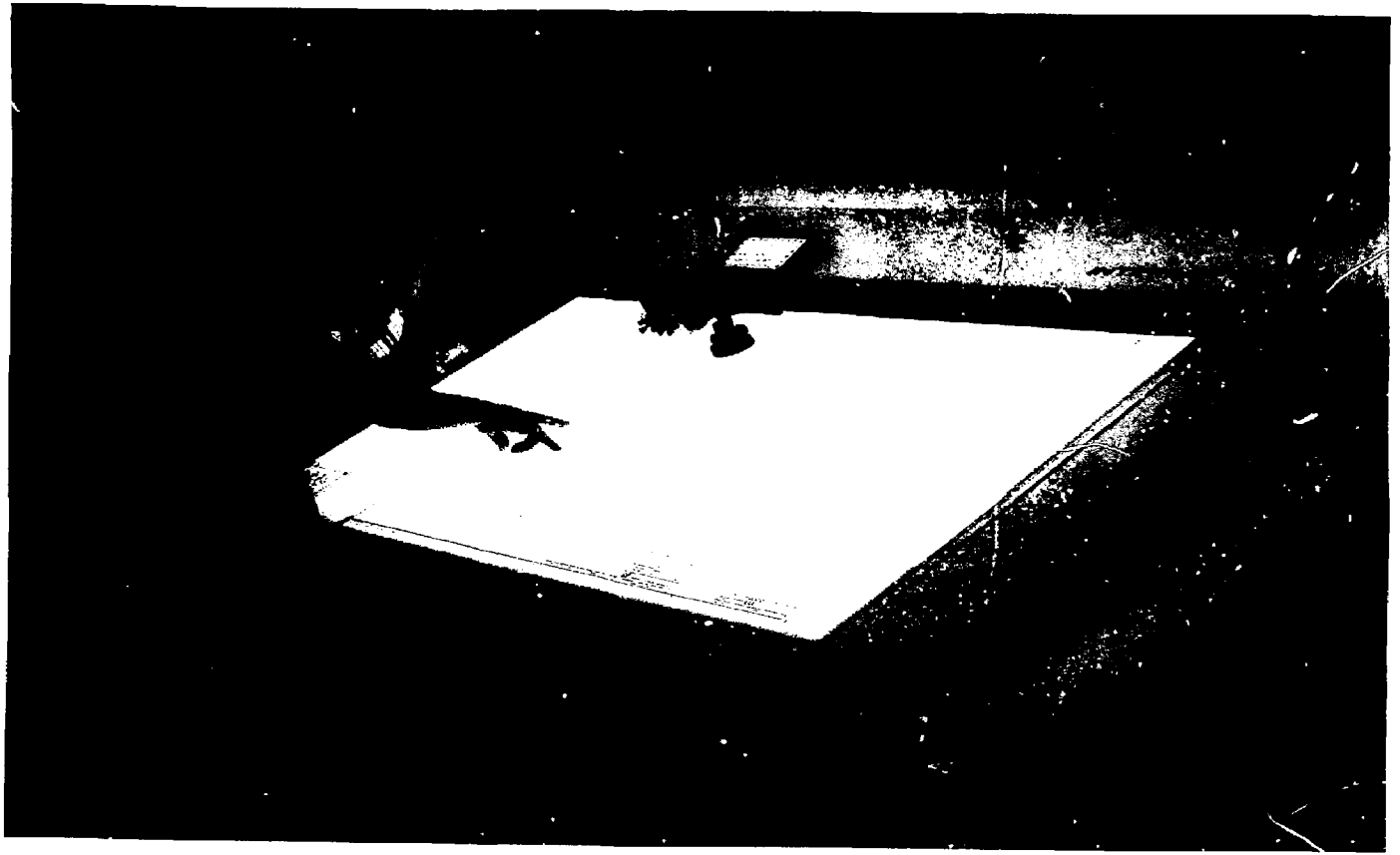

Figure 9. Final Case Structure was Automatically Drafted using CAD.

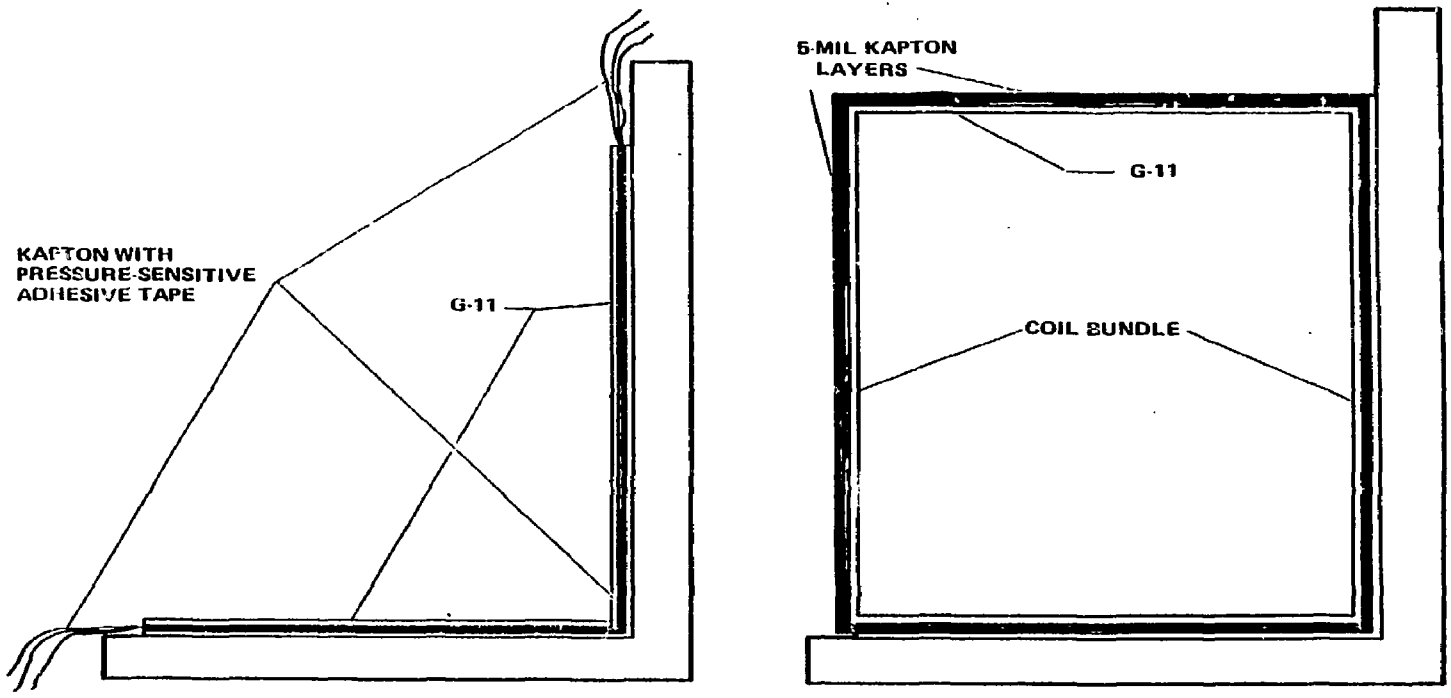

Figure 10. Kapton Corners Facilitate the Coil Winding Operation

A helium plenum is provided above the top surface of the conductor bundle, consisting of approximately forty layers of 1/16 inch thick slotted G-11 laminate. The layers are bonded and the slots are staggered to permit helium passage throughout the entire area while providing for transmittal of coil magnetic forces to the jacket.

Eight inch diameter helium entrance and exit pipes are provided at the low point and high point of the jacket. The helium exit port at the high point provides space for conductor leads to the winding and for routing of instrumentation wiring.

To support the conductor leads, a one inch thick G-11 sheet is installed through the center of the pipe. As shown in Figure 11, brackets on each side of the sheet are installed and clamp the conductor leads on each side of the fiberglass center support. Slots in the center support provide for helium cross flow within the pipe. A six inch helium creepage path is provided by locating the slots adjacent to the outboard edges and having the central portion. The conductor leads are so oriented that magnet forces on the leads result in forcing the leads against the center support.

After the conductor bundle is capsulated with Kapton insulation, the area between the conductor bundle and the jacket cover is filled with a combination of G-11 sheets and an epoxy/chopped glass filler. This transmits the electromagnetic coil forces to the jacket. The combination of G-11 and epoxy provides more than the 6000 psi compressive strength required.

In order to achieve a tight fit of the jacket covers to the coil assembly, the jacket covers are constructed in subassemblies. A "L" section throughout the entire large radius area enables a tight closure against the side and top in that region. A tight fit in the small radius region is achieved by providing a rolled radius side cover and a separate top cover. The side cover, and then the top cover will be fitted in place, and the two pieces will then be tacked and removed for welding into a subassembly.

Jacket close-out welds are designed to prevent damage to the conductor pack during welding. Butt welds are a LLL design which incorporates recessed interior joints and CRES steel back-up sheets. The corner welds incorporate a copper chill bar to distribute the heat and prevent damage to the adjacent materials. Both of these weld joints are shown in Figure 12.

3.1.1 INSULATION. The MFTF magnet is designed for a 1000V potential during a quench condition. Selected insulation materials were reviewed for adequate voltage tracking breakdown capability along dielectric surfaces and for breakdown across gaps in a gaseous helium environment.

Data on the voltage tracking strength of G-11 was not available at 4.5K. However, such data was available on other insulating materials such as mylar, polyethylene, and nylon. Assuming that G-11 is at least as good in tracking strength as the worst of these materials, and using a design safety factor of 10, we have selected a minimum creepage length of 5 cm.

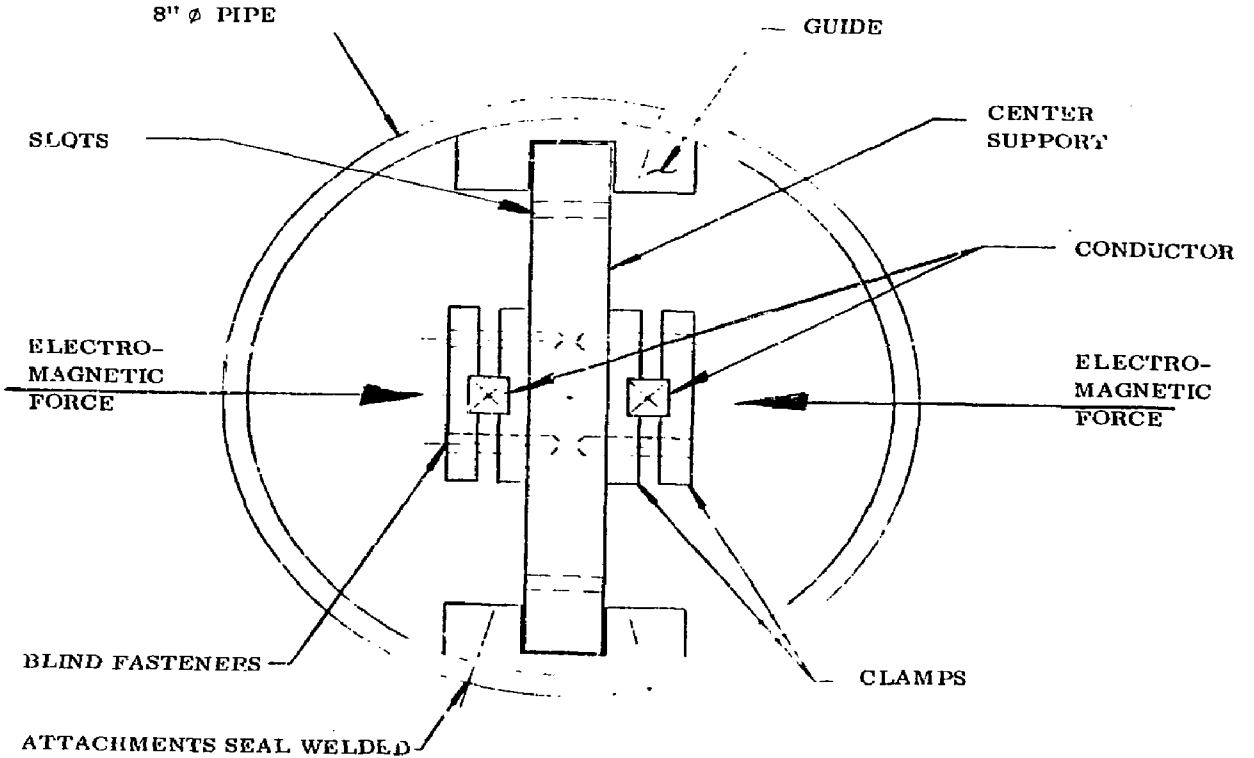

Figure 11. Conductor Leads Have Been Properly Supported

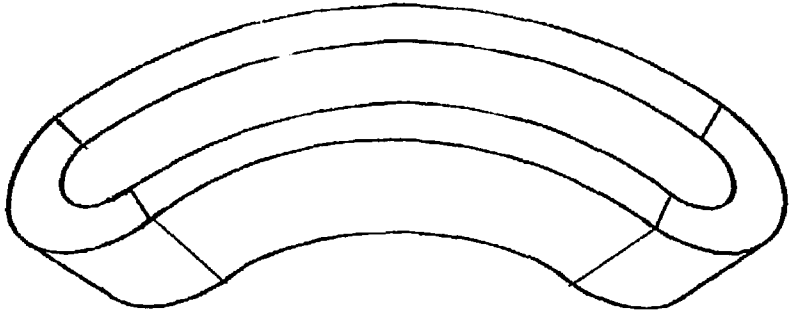

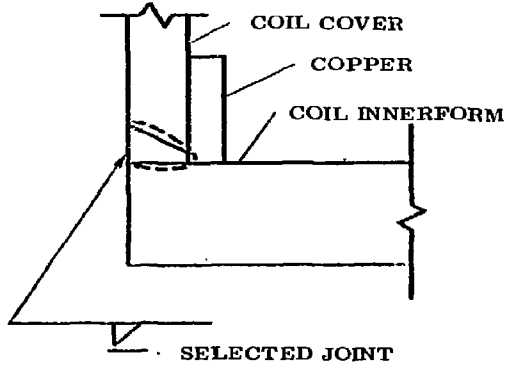

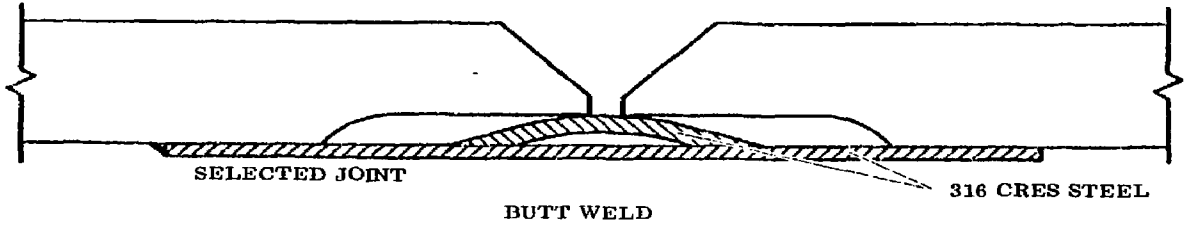

Figure 12. LLL Developed Close-Out Weld Has Been Incorporated in the Jacket Covers

3.1.2 ELECTRICAL. The eddy current heating in the shim bladder represents an energy loss that occurs during a charging cycle. An estimate was made of this heat loss and it was determined that it is less than 1.5 W. This is a maximum value since it was calculated assuming $\dot{B}$ is oriented perpendicularly to the shim bladder cross section.

3.1.3 THERMAL SHIELDS - EDDY FORCES. During a quench, when the magnetic field of the coil has its greatest rate of change, eddy currents will be induced in the 304L stainless steel LN_2 shields surrounding the case.

The LN_2 shield consists of segments which are essentially a rectangular box, approximately 2.6 m by 0.6 m, made of 0.330 cm 304L stainless steel. The magnetic flux through the shield was calculated using field plots provided by LLL, and the rate of change of the flux was determined from the quench characteristics. The total eddy forces were calculated to be 8.97×10^{-4} psi. This force is negligible and poses no threat to structural integrity of the LN_2 shield.

However, if the LN_2 shield were OFHC copper, of the same thickness as the stainless steel, the above calculated force would be multiplied by 220, giving a total force of 0.197 psi. This is almost five times the gravitational load on a copper LN_2 shield, and eddy forces would then have to be considered.

We also estimated the magnitude of the magnetic forces acting on the shields. Normally, the effect of magnetization in 300 series stainless steel is negligible and may be safely ignored. However, the magnetic permeability of 304L stainless steel is highly dependent upon the degree of cold-working. We evaluated the potential magnetic forces induced in 304L and found them to be excessive. We also investigated the alternative shield material, 316L, and found that cold-working has negligible effect. Therefore, since 316L meets all other requirements for the shields, it was selected for MFTF.

3.1.4 ELECTRICAL LEAD INTERFACE - ELECTROMAGNETIC FORCES IN LEADS. The current carrying leads will be affected by electromagnetic forces due to the magnetic field in the vicinity of the exit point at the case. The supporting structure for the leads must be capable of successfully reacting these loads.

The B field values where the leads exit from the case were obtained from field plots supplied by LLL. The definition of local coordinates X', Y', Z' is such as to make Z' parallel to the current carrying leads. The force on a conductor carrying 6000A in the positive Z' direction away from the magnet) has components of $F_{X'} = -18.0$ lb/in and $F_{Y'} = 110$ lb/in, the total force being 111 lb/in. This is the maximum force the lead will experience, since the field decreases as Z' increases.

3.2 CASE DESIGN

The case design incorporates many features developed during the preliminary and final design phases to meet contractual requirements. The case configuration must structurally react magnetic, handling, thermal and seismic loads. Provisions for neutral beam injection windows and clearance for diagnostics are incorporated in the case. The outer case cavity provides a guard vacuum for protection against potential helium leakage. The case material is 304 LN stainless steel with 316L weld filler. This is a revision from the original 21-6-9 stainless steel with inconel 625 weld filler. The configuration of the case facilitates manufacturing and assembly.

To provide the required stiffness and load carrying ability in the case, the final case configuration was revised from the baseline configuration, as shown in Figure 13. The depth of the case cross section was increased by 15%. External case stiffeners and a flange (extension of center plate) were provided to reduce secondary bending moments due to magnetic pressure.

Case thickness was increased in the inner side plate to three inches, and the flat plates in the small radius region, adjacent to the coil cavity, was increased to five inches. The neutral beam injector windows have been maintained. Due to the increased thickness of the inner side plate, the diagnostics window at the center of the small radius was reduced by one inch.

A baffle assembly is provided inside the guard vacuum portion of the case to direct cooldown helium gas along the inner surface of the case, as shown in Figure 14. The impedance of this flow path is essentially equivalent to that in the coil cavity, such that the case cooldown is balanced and the thermal gradient minimized.

Since 304 LN stainless steel is available in wider plates than is 21-6-9 stainless steel. The number of pieces required for the large side plate was reduced. Thus, the required welding and subsequent weld distortion was minimized.

3.2.1 CASE SHIMMING. The jacket to case shim must accommodate the expected uneven gap (due to manufacturing tolerances) between jacket and case, to transfer magnetic loading from jacket to case, and to provide channels in the guard vacuum.

The shim design consists of a 0.04 thick bladder (see Figure 15) which encloses the jacket and coil assembly and is injection filled with urethane. The bladder is formed from annealed CDA 260 copper alloy which was selected for its high ductility and brazability. The splice joint configuration facilitates assembly fit-up and is self fixturing for brazing. Dimples provide a stand-off space for guard vacuum and for cooldown gas flow. Solid disks in 25% of the dimples prevent crushing of the dimples in the event of a tight fit between the jacket and case during fit-up and assembly.

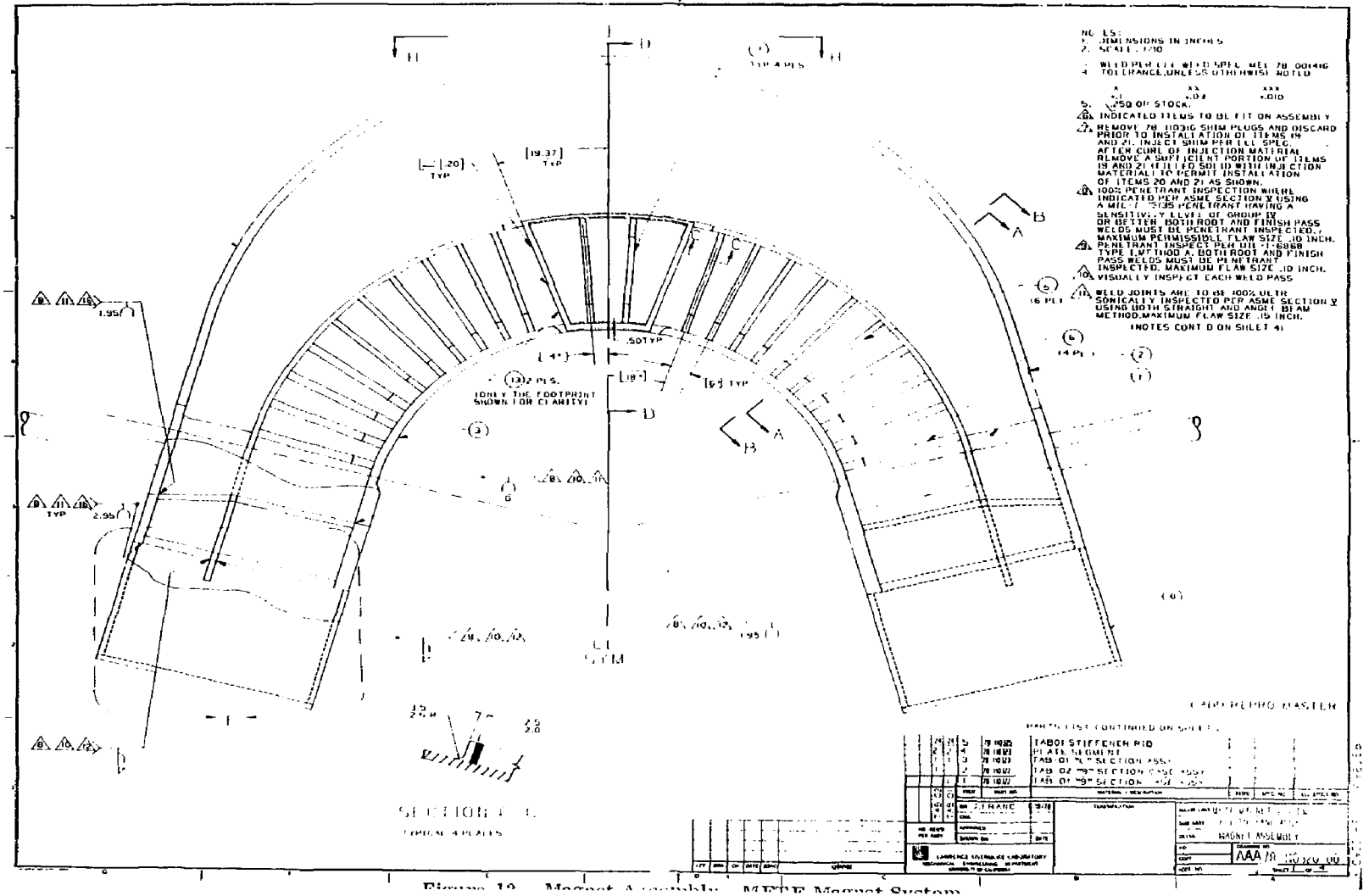

Figure 12. Magnet Assembly, MFTF Magnet System

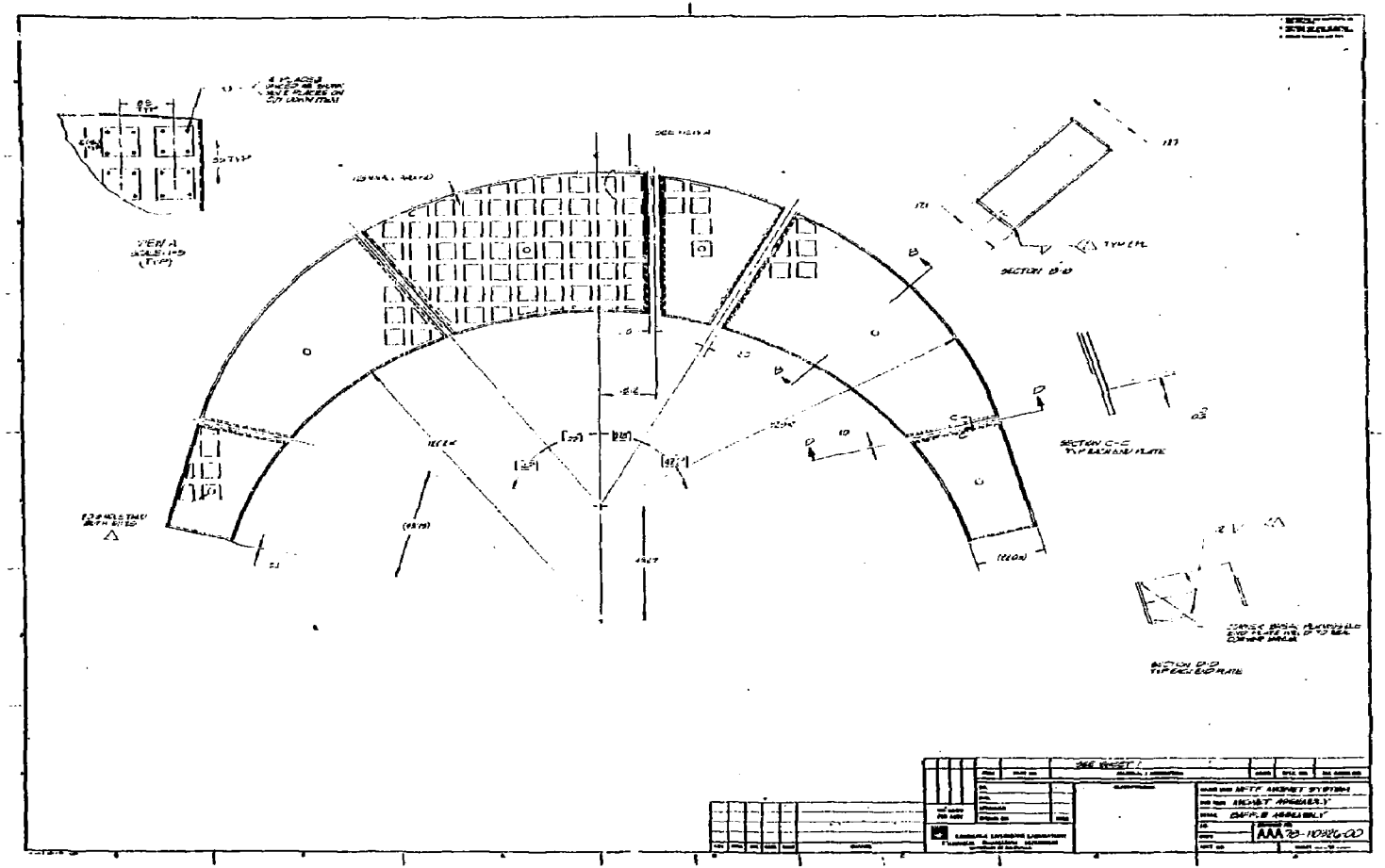

Figure 14. Baffle Assembly – MFTF Magnet System

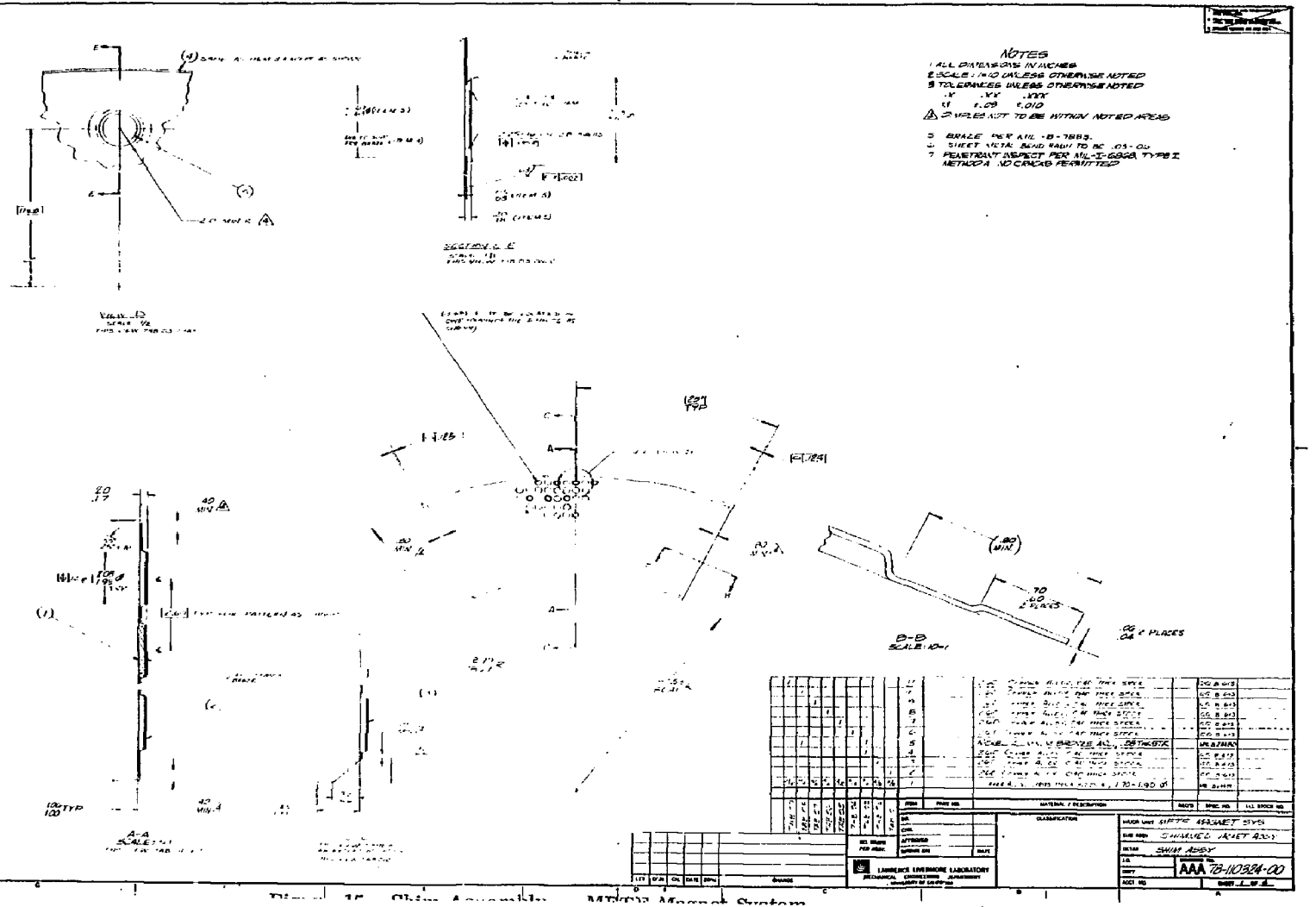

Figure 15. Shim Assembly, MTTR Magnet System

Injection of the urethane will be through two 2-inch pipe connections at the lowest points of the magnet. The vent and overflow ports are also 2-inch pipe and are located at the highest points in the magnet. After the injection material cures, the fill and vent pipes will be cut off and the holes in the case covered and seal welded.

3.2.2 INTERCOIL MEMBERS. The final configuration of the intercoil member is shown in Figures 16 and 17. This highly loaded structure carries 7 million pounds of compression when the magnets are fully energized and is also designed to withstand handling and seismic loads.

The most efficient configuration for the intercoil member was found to be a box arrangement with the top and bottom plates of the box aligned with the case webs to facilitate the distribution of loads from the case into the intercoil member. The side plates of the box are aligned with two webs in the case extension to facilitate the distribution of loads from the intercoil member into the case extension.

Wedges are installed during final assembly to accommodate tolerance buildup and to accurately position the yin relative to the yang magnet. The wedges will be selectively fit on assembly.

Following installation of the wedges, two closure plates are installed to seal up the intercoil structure for cooldown. As shown in Figure 18, helium cooldown gas enters the structure through a single penetration in each extension and is channeled between the extension webs before entering the guard vacuum through an orifice. Only a fraction of the cooldown gas is allowed into the intercoil member in order to control the rate at which the intercoil member cools down relative to the initially warm case to which it mates.

As with the case structure, type 304LN stainless steel material was chosen for the intercoil structure because of its excellent strength characteristics at 4.5°K.

3.2.3 THERMAL SHIELDS. The design of the magnet thermal shielding was a most challenging task from both a technical and schedule standpoint. The shielding requirements resulted in the configuration shown in Figures 19 and 20.

Radiation shielding of the superconducting magnets is provided by a LN_2 shield. This shield completely encloses the magnets and consists of 184 embossed stainless steel 316L panels.

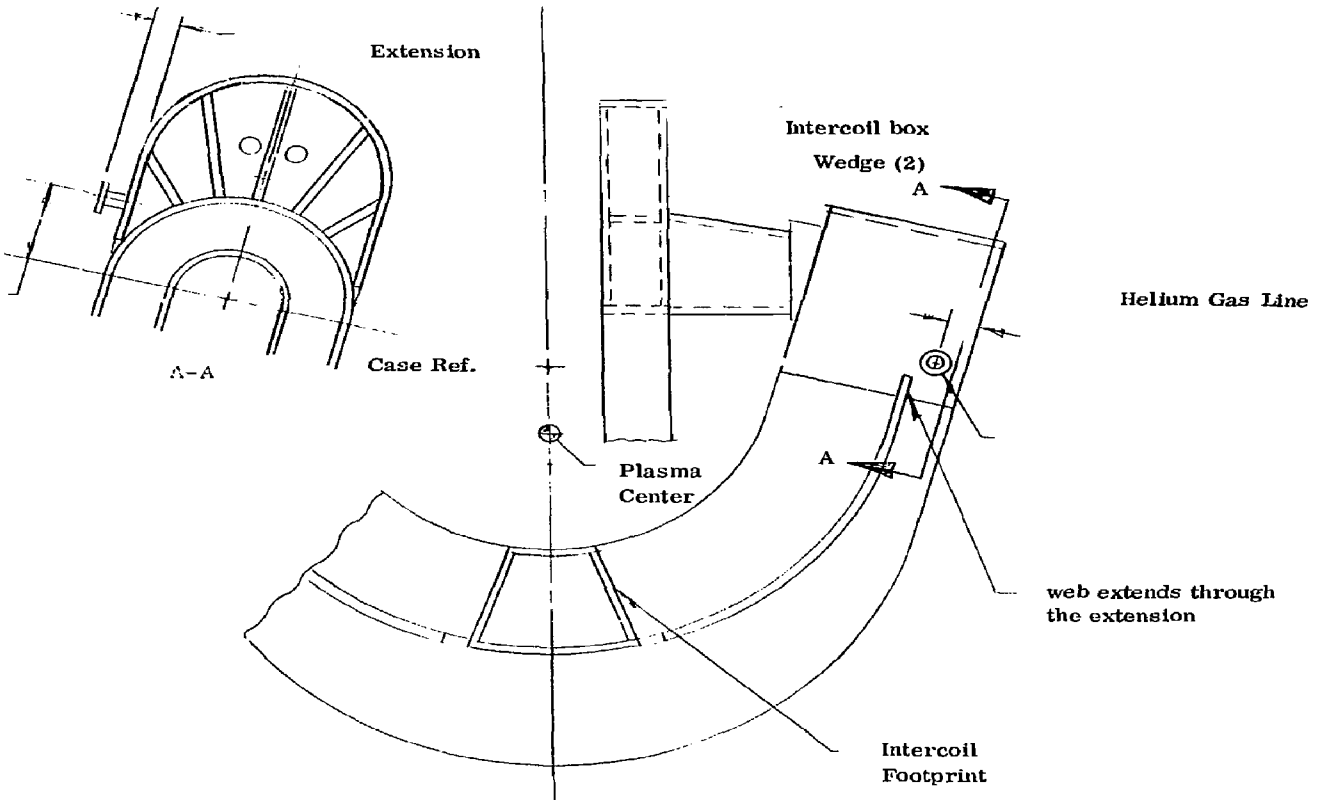

Figure 16. Intercoil Structure

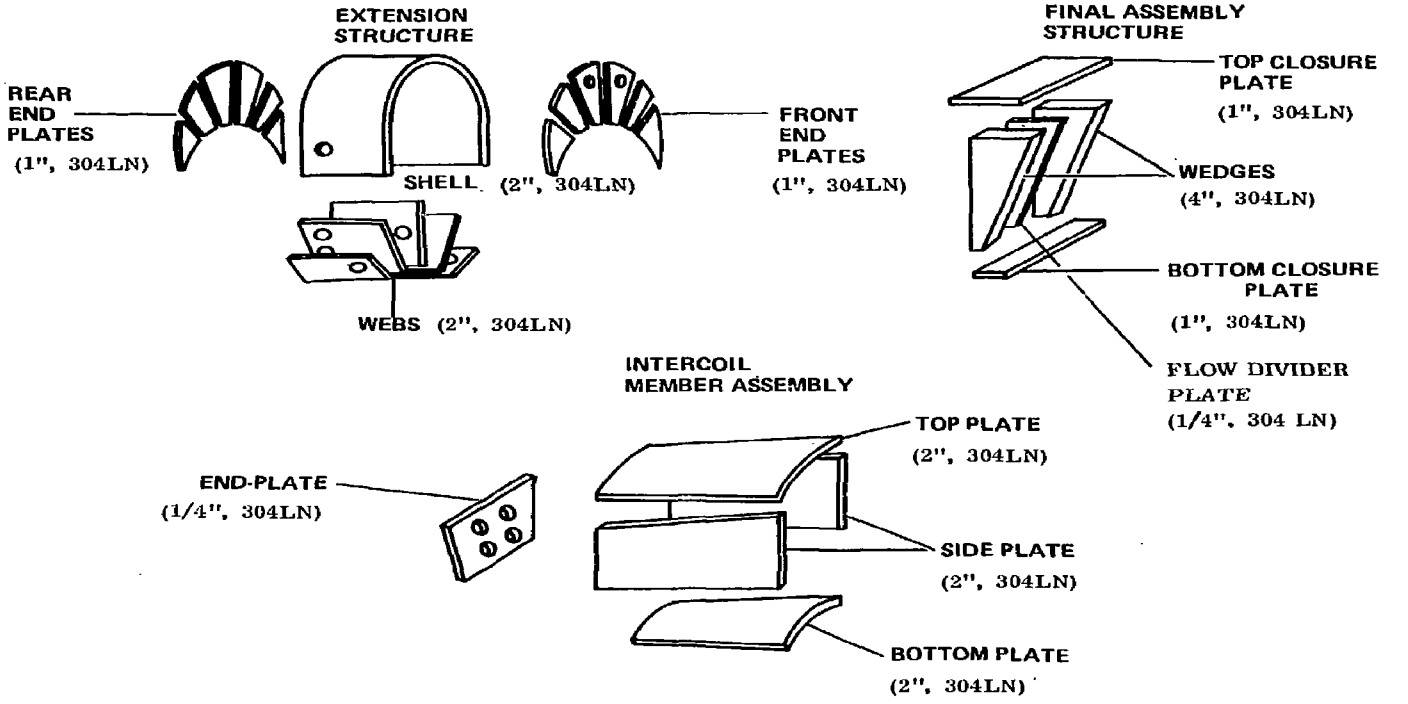

Figure 17. The Intercoil Structure Comprises Three Constituent Structures

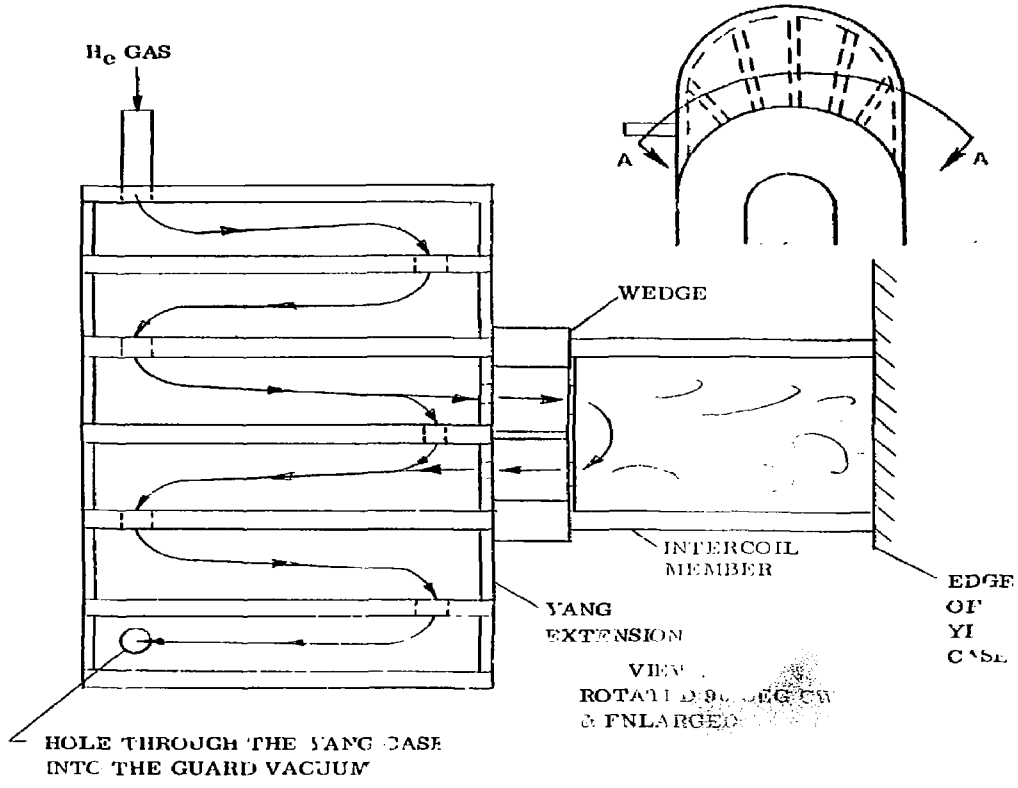

Figure 18 Intercoil Cooldown Test

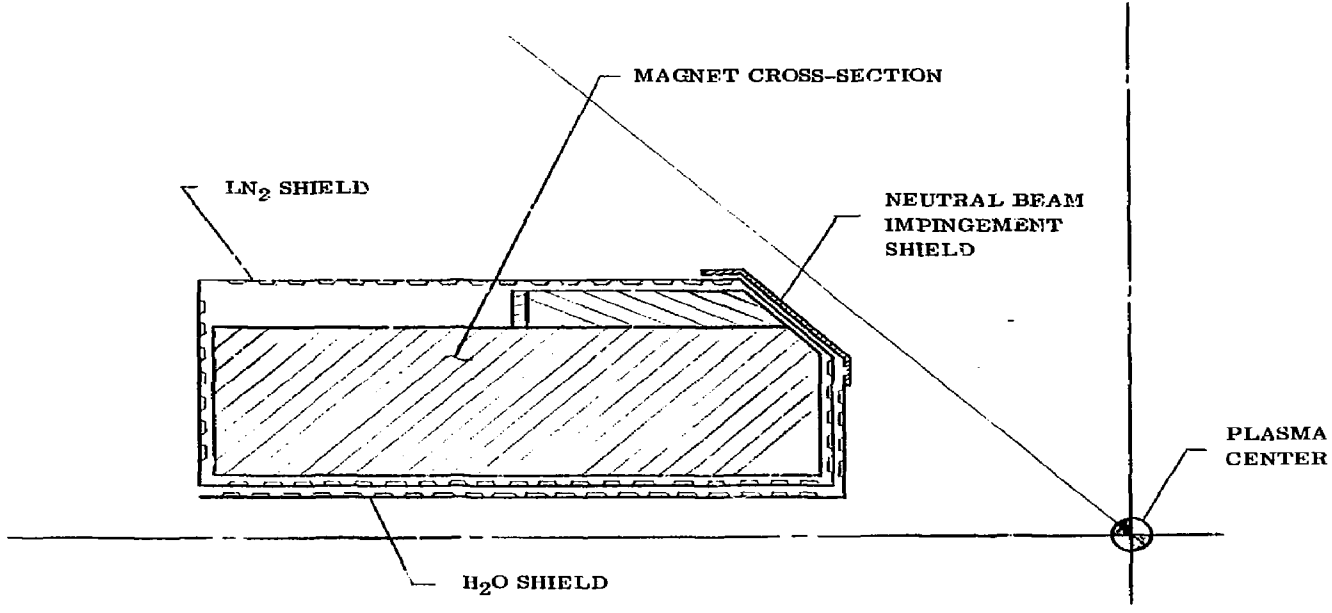

Figure 19. Magnet LN_2, H_2O, and NBI Shielding Arrangement

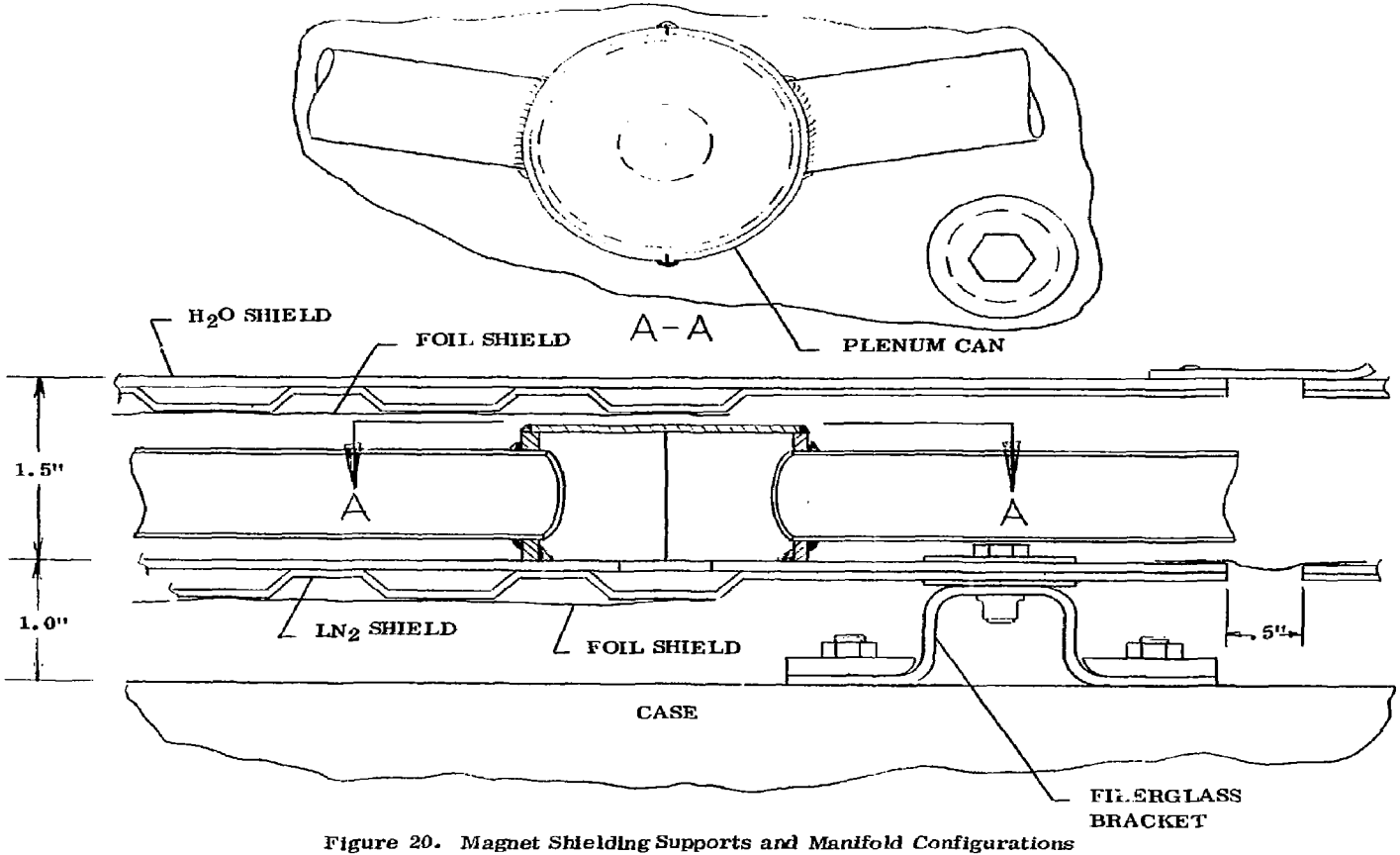

Figure 20. Magnet Shielding Supports and Manifold Configurations

Plasma spatter shielding is provided by an H_2O shield. This shield is provided wherever the plasma can view the surface of the magnets. It consists of 76 embossed stainless steel (316L) panels.

Neutral beam impingement shielding is provided by another H_2O shield. This shield is located along the four chamfered edges of both magnets to protect the magnets from misaligned neutral beams. It consists of high purity (OFHC) copper diffusion bonded to stainless steel. High purity copper is used to minimize plasma contamination.

Three foil radiation shields are provided. These shields are located between the magnets case and LN_2 shield, between the LN_2 shield and the H_2O shields, and around the support rods. The shields consist of 3 mil thick aluminum foil chemically coated per MIL-C-5541B for low emissivity.

The shields are outside the LLL specified stayout zones. These zones are maintained by restricting the shields to a 7/8 inch space at the chamfered edges of the magnet and at the diagnostics window in the minor radii of the magnets. The shields are also restricted to a 4 inch space on the inside legs of the magnets.

All shields are designed to gravity drain. This is necessary to prevent freezing of the H_2O and LN_2 in the event of a coolant circulation failure.

The LN_2 shield and NBI shields are designed to accommodate bubble percolation. This is necessary to prevent the buildup of trapped gas pockets.

Expansion joints are provided in the supply and return manifolding of the shields to accommodate differential thermal expansion of the shields. Supply line and vent line routing for the shields was layed out on specifically designed models as shown in Figure 21.

The use of plenum cans on the LN_2 and H_2O panels minimizes space requirements and simplifies tubing installation. Over 1400 fiberglass (MIL-C-9084C) brackets are used to support the shields. The LN_2 shield fittings and the H_2O shield fittings are staggered to minimize the heat leak to the magnets. Fasteners, through oversized holes in the panels, attach the shields to the fittings. The oversized holes with spiral expansion springs accommodate differential thermal expansion of the shields.

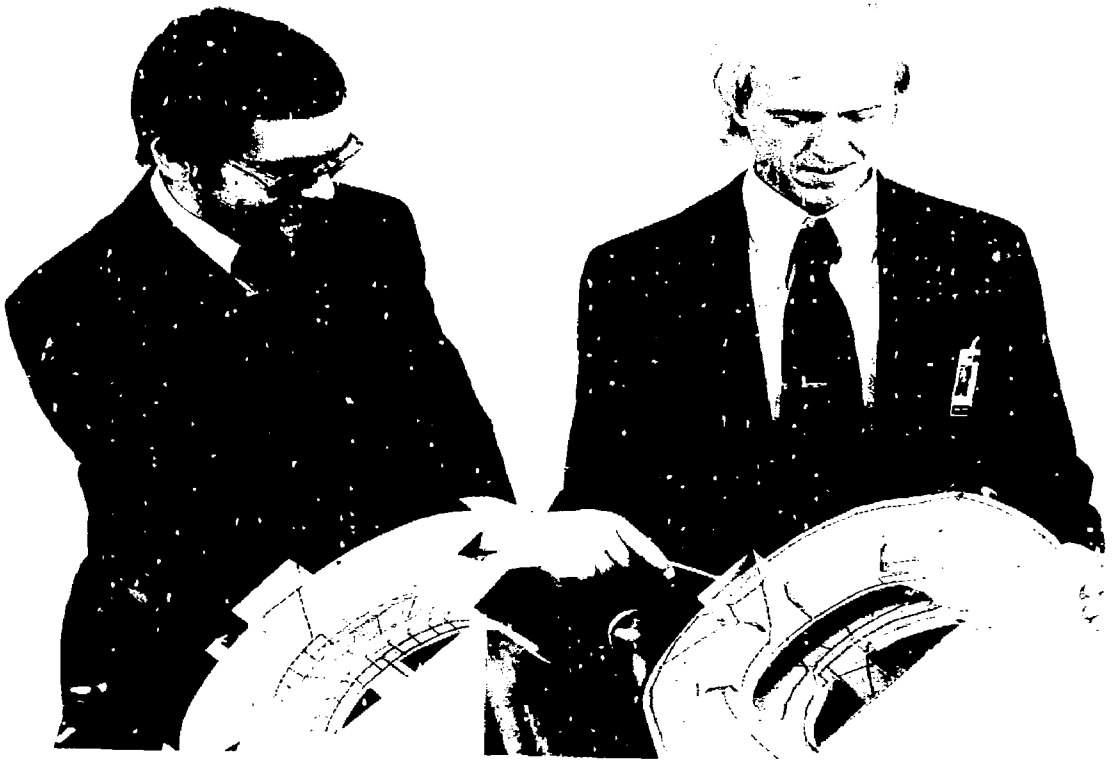

Figure 21. Engineering Mock-Ups of the Shields and Manifolds Systems Aided Design

3.3 SUPPORT STRUCTURE

The support structure, as shown in Figures 22 and 23, has evolved as a result of continuous re-evaluation and change during the design phase.

All stabilizer rods were designed to take compressive loads in order to fully stabilize the magnets during an earthquake. This was done by having spherical bearings at the rod ends for universal joints and by using 10 inch diameter pipe for the rods (was 5 inch diameter round) to prevent column buckling of the rods.

The hanger rods were changed to the same design as the stabilizer rods to provide a common design of the rods.

Liquid nitrogen sleeves were added to the hanger and stabilizer rods to limit the heat leak through them. These sleeves were found to provide the maximum benefit when placed 20 inches from the end of the turnbuckle, on the end closest to the magnets.

A foil radiation shield was added to all the support rods to minimize heat transfer from the warm inner surfaces of the vacuum vessel.

End pins were resized for the latest configuration and loads.

Dry film lubricant (Everlube 811) was added to the turnbuckle threads to minimize the torque required to adjust the support rods.

Both A286 and 304L stainless were employed in the design of the support rods. These dissimilar materials prevent galling at all bearing surfaces.

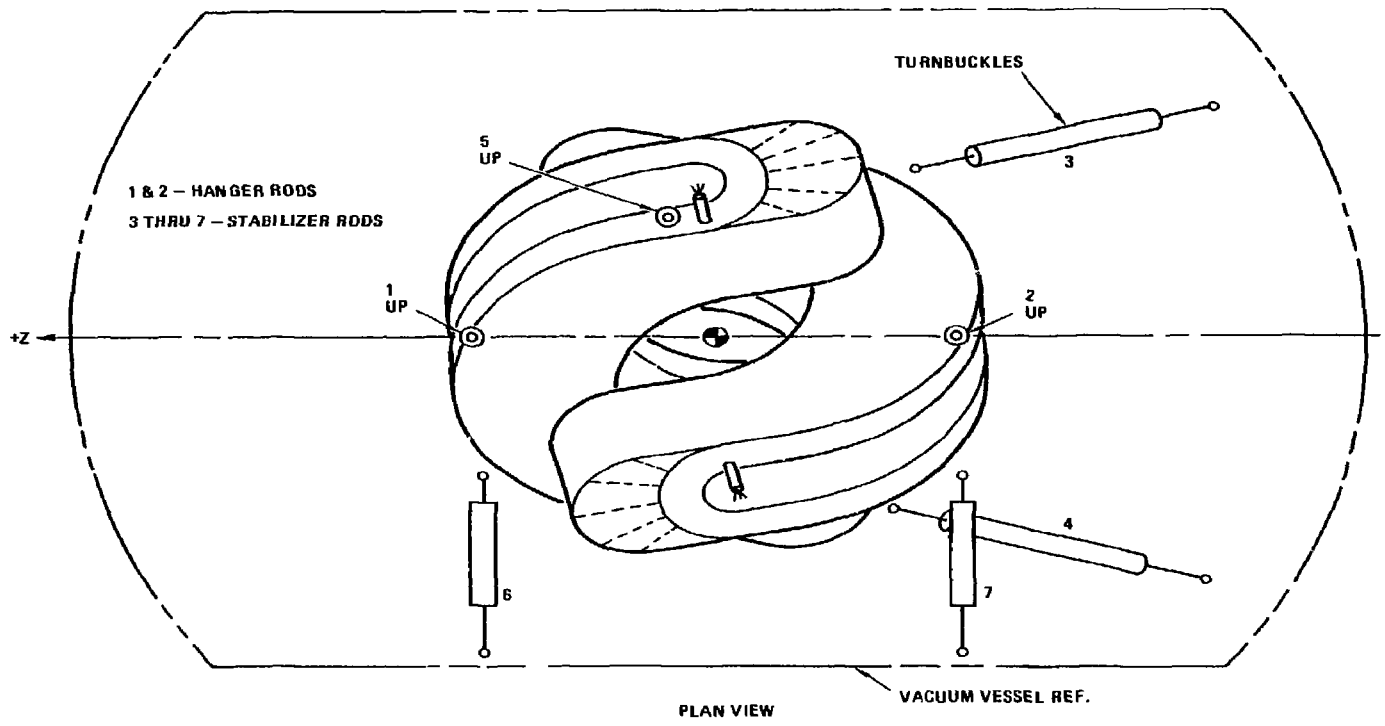

Figure 22. Hanger & Stabilizer Support Rod Configuration (Plan View)

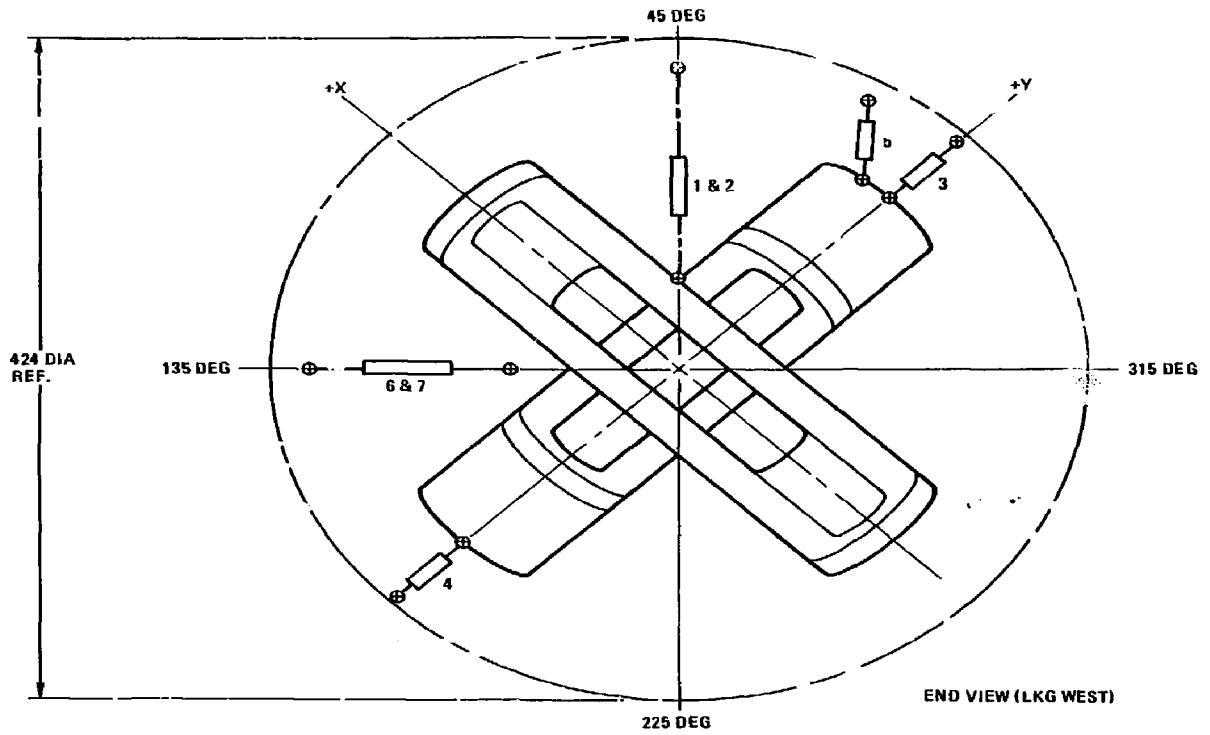

Figure 23. Hanger & Stabilizer Support Rod Configuration (End View)

4

INSTRUMENTATION

MFTF instrumentation requirements, defined by LLL, included preliminary allocations of 100 strain, 100 temperature and 80 voltage channels with an upper limit of 300 channel monitoring capacity. These measurements required that 1) strain gages be located to confirm stress analyses, 2) temperature sensors be positioned for monitoring cooldown to safely limit thermal stresses, 3) temperature sensors be provided which monitor the magnet to ensure safe and proper operation and 4) voltage taps to be located in the coils for monitoring conductor resistance during operation in order to detect normal zones.

After a number of iterations throughout the design and analyses phases, final instrumentation measurement quantities and locations for the MFTF magnet system were established. The three basic categories of measurements utilized, which are voltage, strain, and temperature, have been placed in key locations to fulfill the program requirements. A summary of the quantities and general locations of these measurements is presented in Table I. The total of all measurement installations is 271 channels, which include 44 voltage, 114 strain, and 113 temperature locations. A final measurement list was prepared which includes each individual measurement description keyed to its sensor location drawing and drawing number, along with its associated measurement range, units, transducer description, and part number.

Instrumentation measurements were located and selected to provide strain and temperature monitoring data on coil No. 1 and No. 2 jackets, cases, intercoil members, and support rod turnbuckles for magnet cooldown and warmup performance. This data may also be utilized to verify strain/temperature analyses, and provide manual control data if deemed necessary by high stress or temperature gradient indications.

The cooldown/warmup strain and temperature sensors that are located on the magnet case and jacket plates throughout various locations are depicted in Figure 24. As can be noted, some sections contain both strain gages and temperature sensors, while other sections contain only strain gages or temperature sensors. Gages are typically located near the four corners of a case section, as denoted by A, C, D and F on the cross sectional view. Some sections are more heavily instrumented than others to provide additional data on stiffeners or extension plates. A total of 87 strain and 54 temperature sensors are located among all the sections noted. The +X and +Y (magnet local axis) intercoil members each have ten strain and two temperature sensor locations. Rosettes are mounted on two sides of each intercoil for determination of shear data in addition to the axial strains. The temperature sensors provide for correlating temperature/strain data. One strain gage and one temperature sensor are installed on the turnbuckle of each support rod and stabilizer to provide axial

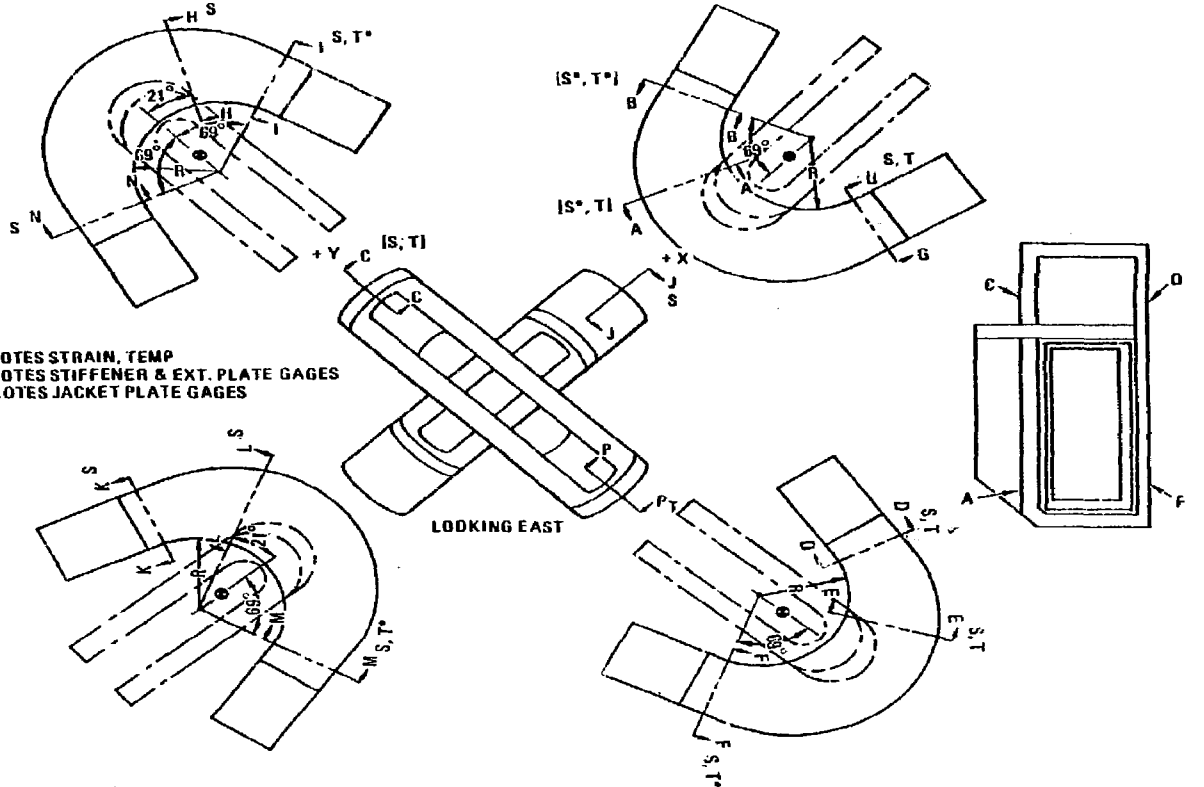

Figure 24. Case and Jacket Cooldown Strain and Temperature Sensor Locations

Table I. MFTF Measurement Summary

Type	General Location	Measurement	Redundant Installations
Strain	Case Plates	75	
	Jacket	12	
	Support Hangers and Stabilizers	7	
	Intercoil Structure	20	
		114	
Temp.	Case Plates (Cooldown)	46	
	Jacket (Cooldown)	8	
	Case (Operational)	16	
	Thermal Shields (Operational)	16	16
	Support Hangers and Stabilizers	7	
	Intercoil Structure	4	
		97	16
Voltage	Coil No. 1	14	
	Coil No. 2	14	
	Coil No. 1 Current Leads	4	4
	Coil No. 2 Current Leads	4	4
		36	8
	Total Measurements	247	24
	(Grand Total of 271 Channels)		

strain and correlating temperature data. The strain gage will determine support system loading during rigging, system load changes during magnet operation and system loads during seismic excitation.

Operational measurements include voltage tap measurements above and below each current lead splice and in each coil bundle at every fourth layer. In addition, temperature sensors are provided on the inner surface of neutral beam thermal shields and on the magnet cases behind the thermal shields at each neutral beam entrance and exit location. These data will provide thermal shield control and magnet case thermal protection.

Instrumentation drawings were prepared to locate and install the various sensors throughout the magnet system. A drawing tree for these is shown in Figure 25.

A summary of all sensors selected is provided in Table II. Strain gages and temperature sensors were selected based upon the measurement application. The strain gages were LLL selected after extensive testing for determination of apparent strain curves resulting from thermal and magnetic effects.

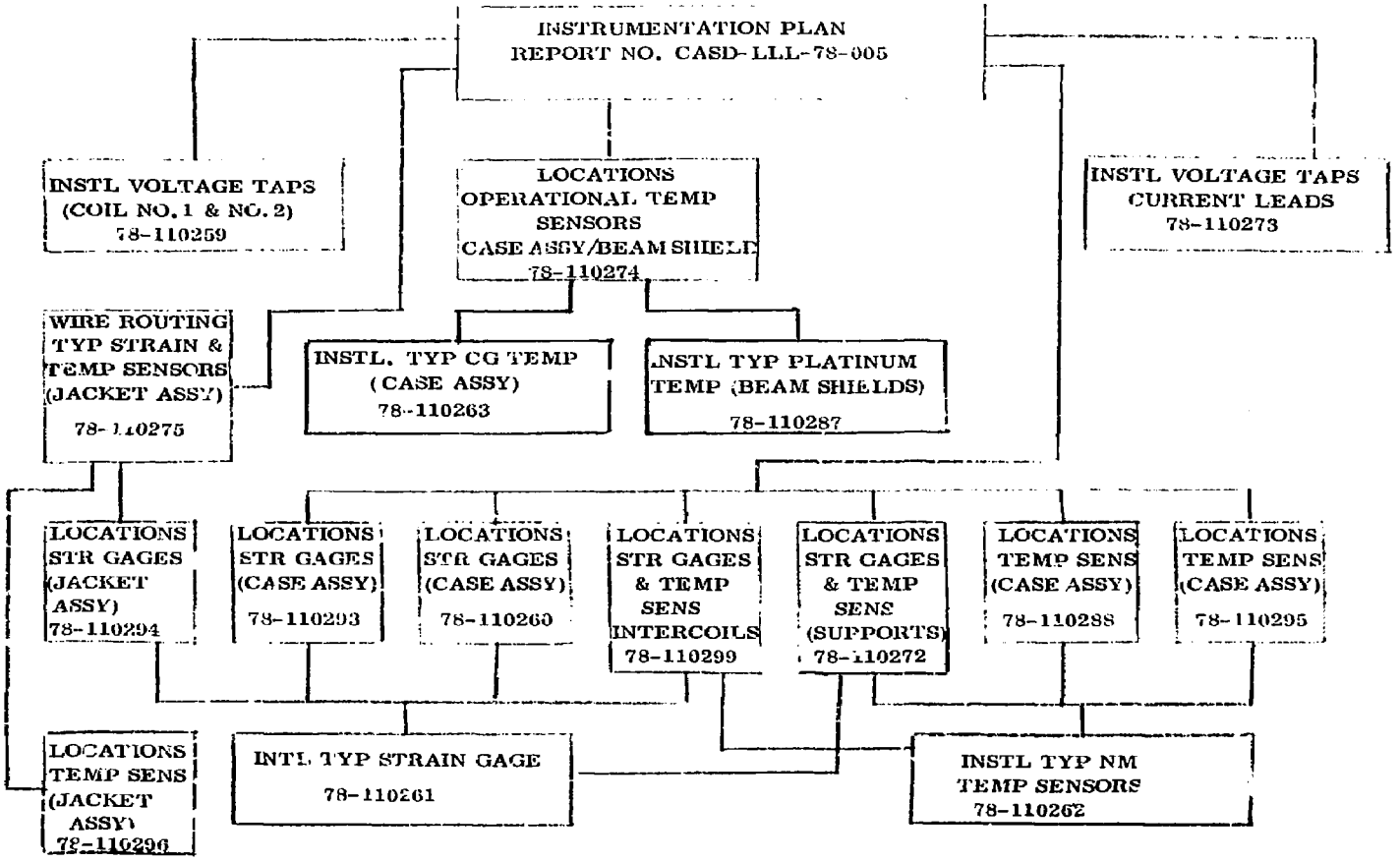

Figure 25. *MFTF* Instrumentation Drawing Tree

Table II. Sensor Selection and Rationale

Measurement Type	Sensor Data	Selection Rationale
All Structural Strains	Type - Metal Foil Strain Gage P/N - WK-15-250-BG-350 Range - ± 4000 MST MFG - Micromeasurements	LLL Selected and Tested for Thermal and Magnetic Field Effects
All Structural Cooldown Temperatures	Type - Nickel - Manganin Resistance P/N - CLTS-2 Range - 300 to 4.2° K MFG - Micromeasurements	Linear Output Over Wide Temp. Range Sensitivity - ΔR = 700 ohms
All Case Operational Temperatures	Type - Carbon Glass Resistor P/N - CGR-1-1000 Range - 4 to 10° K MFG - Lakeshore Cryotronics	Minimum Magnetic Field Effect High Accuracy
All Neutral Beam Thermal Shield Temperatures	Type - Platinum Wire P/N - 118MG100A Resistor Range - 280 to 540° K MFG - Rosemount	Linear Output Over Wide Temp. Range Sensitivity - ΔR = 100 ohms

5

MATERIALS AND PROCESSES

Materials and Processes supported the MFTF Program in four major areas:

1. Provision of existing applicable specification, codes and standards.
2. Selection of materials,
3. Provision of data on selected materials, and
4. Review of design drawings.

Upon initiation of the MFTF Program, copies of all of the applicable specifications, codes and standards which were mentioned in the RFQ were made available to the MFTF analysis and design personnel.

During the preliminary and final design phases of the MFTF program, recommendations were made for selection of metallic and non-metallic materials for the MFTF case, jacket, shields and support structures. These recommendations are summarized in Table III.

One of the more significant contributions was in the selection of structural materials for the MFTF case. Substitution of nitrogen strengthened Type 304L austenitic stainless steel (304 LN) for 21-6-9 stainless steel (Nitronic 40) was recommended. This cost savings suggestion was made possible by the recent work of the National Bureau of Standards (NBS) summarized in Figure 26 which shows the effect of nitrogen on yield strength of 304L at room and cryogenic temperatures.

In addition to the structural materials, recommendations were also made for the selection of organic fillers and adhesives. Ease of application and reliability at cryogenic temperature (4° K) were the main selection criteria. Many commercially available materials may have been acceptable, however in the absence of verification testing, selection was based on available data or General Dynamics experience with the materials at cryogenic temperature. The recommended materials and the applications are listed in Table IV.

Mechanical and thermophysical properties at room and cryogenic temperatures, processing information, availability and cost data on the selected materials were provided to MFTF designers and analysts. This information was recorded in the "Energy Systems Project Design Manual, Book I - Materials Properties."

All of the MFTF design drawings were also reviewed and signed-off.

Table III. Recommended Materials Selections

WBS 3000 Jacket	Specification
316 CRES Stl Plate 1/2", 1"	SA 240 Type 316
316 CRES Stl Bar 1" × 1", 1" × 1-1/2	SA 479 Type 316
316 CRES Stl Rod 1/2" Dia.	SA 479 Type 316
CDA - #464 Naval Brass Roc 1/2" Dia.	
1/32" Fiberglass Sheet	MIL-P-18177 Type GEB
8" SCH 40 S (CRES) Pipe	ASTM A312 Grade *
16" SCH 40S (CRES) Pipe	ASTM A312 Grade *
Epon 828 Epoxy Chopped Glass	
5 MIL Kapton Film	MIL-P-46112 B
316 Weld Rod	ER 3166
Glass Cloth — Fiberglass Layup R.T. Cure	
Resin	
WBS 4100 Case, WBS 4200 Shim	
304 LN Plate (2" - 5")	
316 L Weld Rod	AWS ER 316L
WBS 4100 Shim	
CDA - #360 Copper Alloy (0.040)	QQ-B-613
CuP Braze Alloy - B-CuP-5	AWS A58-69
304L/316L Sheet/Plate (0.20)	SA240 Type 304L/316L
304L/316L Bar (4" Dia)	SA479 Type 304L/316L
316L Tube 4" O.D. × 0.020 Wall	SA213 TP 316L
WBS 4300 Intercoil	
304 LN Plate 2"	
304 L Plate 1/4", 1/2", 2-1/2", 4"	SA240 Type 304L
304L Pipe 4° SCH 405	SA312 Grade TP 304L
WBS 4400 Thermal Shields	
C10100 - CDA 101, 102, 110 Copper 0.30 Sheet	
304L 14/16 6A	SA 240 Type 304L
181 Fiberglass Cloth w/828 Epon Epoxy - Fiber Reinforced Phenolic	
Iridited Aluminum Foil	
Silver Braze (furnace)	B Ag - 8.8a or 19 AWS A5.8 - 69

* Depends on pressure.

Table III. Recommended Materials Selections (Cont'd)

WBS 5100 Support Structure	Specification
304L 5" Dia Bar	SA 479 Type 304L
A 286 4-1/4" Dia & 7-1/2" Dia Bar	AMS 573*
A 286 0.048 Sheet	AMS 5525
Solid Film Lubricant (For Threads)	
WBS 5400 - Bonding and Sealing Adhesives for Strain and Temperature Gages	
Product	**MFG**
M Bond 600	Micromeasurements
AE-15	Micromeasurements
#2850 FT	Emerson & Cuming

* Solution treated

Table IV. Fillers and Adhesives Recommended for Applications

Item	Application	Material Recommended	Process
Fillers	(1) Correction for surface uneveness and out-of-tolerance dimensions of the coil winding form.	Chopped fiber-filled epoxy (Epon 828/versa-mid 125 curing agent and chopped glass fibers	• Trowelled onto the coil winding form
	(2) Jacket-to-coil shimming	Chopped fiber-filled epoxy (Epon 828/ versa-mid 125 curing agent and chopped glass fibers)	• Epon 828 system trowelled onto the coil winding • Stainless steel winding jacket is weld-closed to encase the coils
	(3) Jacket-to-shimming	Two-part, low viscosity, long work life, high compressive strengths and modulus urethane resin (polycast 1009-78 or equivalent).	• Injection filling through the case port-holes to attain tight jacket-to-case-shimming

Table IV. Fillers and Adhesives Recommended for Applications (Cont'd)

Item	Application	Material Recommended	Process
Adhesives	(1) Bonding of ground insulation		
	• G-11 to G-11 epoxy/glass laminate	Urethane adhesive (3M's EC3549 A/b)	• Two-Part adhesive mixed and cured at R.T. bondline thickness is controlled by nylon monofilament or scrim
	• G-11 to filler/ winding form	Urethane adhesive (3M's EC3549 A/b)	• Two-part adhesive mixed and cured at R.T. bondline thickness is controlled by nylon monofilament or scrim
	• Kapton to filler/winding form	Urethane adhesive (3M's EC3549 A/b)	• Two-Part adhesive mixed and cured at R.T. bondline thickness is controlled by nylon monofilament or scrim
	• Kapton to Kapton	Silicone pressure-sensitive transfer tape adhesive (Dennison Mfg. Co., Densil #2078)	• Remove the release backing and apply contact pressure to accomplish bonding
	(2) Bonding of insulation blanket to thermal shield	Two-part, low outgassing epoxy (Hysol's EA934 A/B)	• Two-part adhesive mixed and cured at R.T.

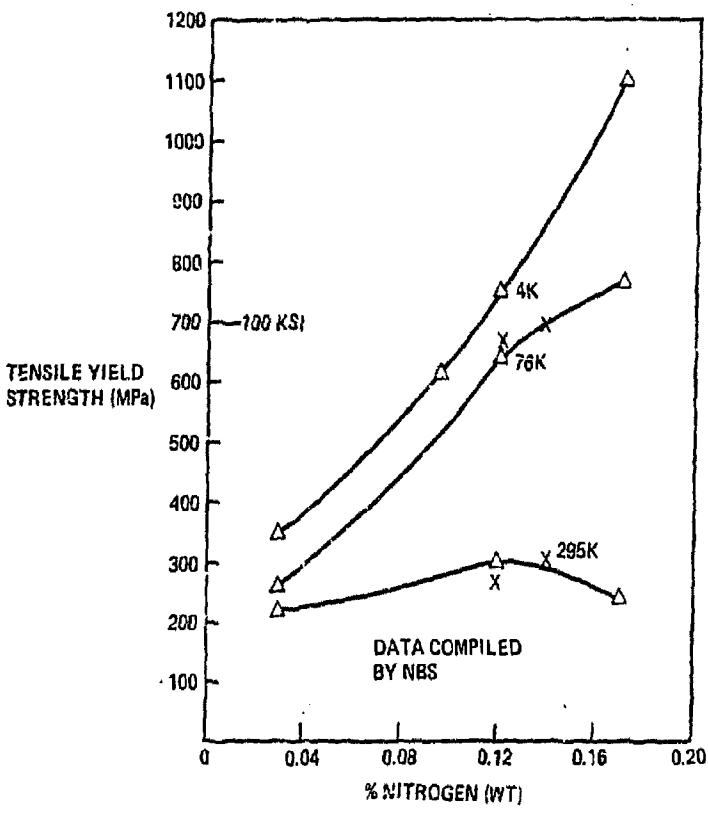

Figure 26. Low Temperature Yield Strength of Type 304L Stainless Steel is Dependent on N_2 Content

6

PRODUCIBILITY

The manufacturing prodicibility requirements for the MFTF magnet system program were to produce a design that could be manufactured economically with existing technology, a design that could be competitively bid, and drawings that fabricating shops could work to. A primary objective of this project was to provide manufacturing engineering direction and guidance to MFTF design engineers in process selection, material requirements and allowances for forming, machining, and welding. A major contribution to this program was the development of a manufacturing assembly sequence and flow plan which defined all major operations required to manufacture and instali the magnet system into the vacuum chamber at the Lawrence Livermore Laboratory. The following are some of the highlights of the manufacturing producibility accomplishments for this program.

Six welding processes were studied for application on the coil case.

1. GTAW - Gas Tungsten Arc Welding (also called TIG, Tungsten Inert Gas)
2. SMAW - Shielded Metal Arc Welding
3. GMAW - Gas Metal Arc Welding (also called MIG, Metal Inert Gas)
4. FCAW - Flux Core Arc Welding
5. ESW - Electro Slag Welding
6. SAW - Submerged Arc Welding

Our study showed GTAW, SMAW, and GMAW to be the processes with the most versatility and economical advantages for the coil case. Our study of the baseline design showed a savings of 7,084 pounds of filler metal and 10,349 manhours could be made by maximizing the use of GMAW welding process instead of SMAW. The FCAW, ESW, and SAW welding process may have limited application on the coil case, but the cost of verification and certification of these processes could not be justified in our opinion. To economically manufacture the case, GTAW, SAW and GMAW welding processes will be required. However, GMAW should be used wherever possible to maximize savings possible with this process.

Detail studies were made of the various weld joint geometries to check welder accessibility, weld filler metal volume, and ease of manufacture. A weld joint geometry consisting of "J," double "J," and "U" joints that would accommodate any of the welding processes studied (except electro slag) were incorporated into our design for the coil case structure. These weld joint geometries would also allow fabricators some latitude in selecting the welding process that best suits their facilities and equipment.

Various methods of cutting the perimeters of detail parts from thick 304LN stainless steel were studied. Our approach of plasma arc cutting the detail parts 1/8-inch oversize, then milling the parts to net size, will save thousands of dollars in machining time. Plasma arc cutting tests run at General Dynamics in 1977 demonstrated that bevel cuts up to 35 degrees could be made in 304 stainless steel three inches thick with conventional equipment.

We recommend that cuts for weld joint configurations be rough plasma arc cut on an angle then subsequently machined to net dimension. This cutting procedure will significantly reduce machining time and cost for this project.

The welding sequence and mating of the "9" and "L" structural assemblies are the most critical manufacturing operations for this project. Weld distortion and tolerance control for these assemblies weighing several tons were given special attention from detail part fabrication to subassembly, to final assembly, to assure fit on final assembly. Manufacturing engineering made a major effort to develop an assembly approach that accommodates and minimizes weld distortion and tolerance build-up where possible, and to reduce rework at final assembly. Our manufacturing sequence for the case is shown on the manufacturing sequence and flow chart in the back of this report, and was approved by LLL personnel at our final design review. This assembly sequence gives the fabricators an opportunity to minimize mismatch and other problems anticipated at final assembly.

The need for a weld and final assembly fixture for the coil case was identified early in the program by our manufacturing engineering team. A conceptual drawing and the requirements for this fixture were developed. The basic function of this fixture is to locate the major components of the coil case and to rotate them into position for downhand welding, also to position the finished coil assembly for mating coil no. 1 to coil no. 2, and the installation of the inner coil members. This tool will reduce handling and welding time at the fabricator's plant, and can be used for shipping the "9" assembly to LLL. It will also be used at LLL to position the "9" and "L" assembly for making the closeout welds.

The need was identified for a cradle fixture for holding coil no. 1 and coil no. 2 after mating, and a conceptual drawing and the requirement for this tool were developed. Basically, this tool would position the two coils for installing the shields and interconnecting hardware outside of the vacuum chamber. The major function of this tool is to provide means for installing these coils into the vacuum chamber, positioning them relative to the plasma center, and to provide location and adjustment of the support rods that connect this structure to the vacuum vessel.

A major contribution to this program was the early development of the manufacturing sequence and flow plan, which is the roadmap that defines all major operations required to produce this magnet. To enhance this development, we also constructed a 1/20 scale model of the MFTF magnet system as shown in Figure 27. This model in conjunction with the manufacturing sequence and flow chart, served as excellent

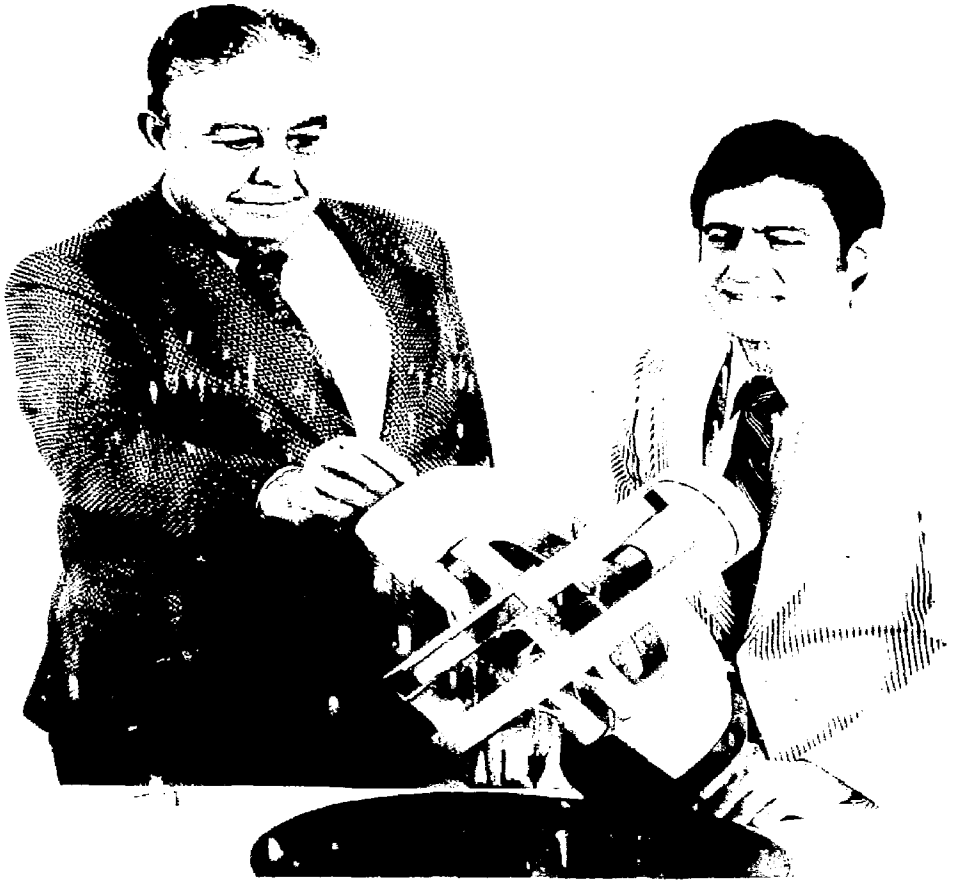

Figure 27. Scaled Mock-Ups Aided Development of Manufacturing Sequence & Flow Plan

tools for LLL and Convair engineers to evaluate design options. The manufacturing sequence and flow plan will also be a valuable tool for briefing potential bidders and to assist them in understanding the critical points of inspection and fabrication of this complex structure.

7

QUALITY ASSURANCE PROGRAM REVIEW

The Quality Assurance activities for the MFTF magnet system started with the initial receipt of the request for proposal. Upon acceptance of the General Dynamics Convair proposal by Lawrence Livermore Laboratory, the Quality Assurance function provided program management support and actively participated in Design and Producibility Planning Reviews. At this time, preliminary inspection methods were established for fabrication and assembly of the Mirror Fusion Magnet System. Each drawing was thoroughly reviewed by Quality Assurance for completeness, inspectability and proper call out of inspection requirements.

The initial Quality Assurance efforts prior to Preliminary Design Review (PDR) included:

Quality Assurance input to manufacturing inspection sequence and flow plan

Material quality requirements to design and stress

Evaluation of NDE methods for inspection of individual weldments

Participation in design and producibility trade studies

Quality Assurance support for fracture analysis study

The results of these activities were presented at the PDR. At which time, discrete areas of concern were identified. They were:

Inspectability of some close-out welds

NDE-Ultrasonic standards to be developed by LLL

Control of dimensional tolerances of original plate material and distortion from welding

Application of strict quality control on materials, welding and personnel and process certification

During the final design phase, close coordination was maintained with LLL MFTF technical staff in finalizing Quality Assurance requirements and the need for refinement of existing LLL specifications.

Reliability Engineering was assigned the task of evaluating the designated instrumentation sensors redundancy for stress, thermal and electrical measurements. After coordinating with the responsible Design Groups, Reliability Engineering Department conducted a reliability redundancy analysis to verify that the recommended sensors provided adequate redundancy for the critical applications. It was concluded from this study that adquate redundancy has been provided.

The Final Design Review (FDR) was held in San Diego on 18 September 1978. During this review the changes made in the manufacturing sequence were discussed as they pertained to inspection of close-out weldments. Special emphasis was placed, during the FDR, on the critical stress areas of the case and support structure and special NDE requirements to support these areas as detailed on the drawing.

Quality Assurance expressed a concern regarding the ultrasonic quality level of the 304LN plate material. Since industry has had little experience with material in the heavy plate thicknesses, ultrasonic inspection was recommended, primarily for delaminations or gross defects. This inspection should be accomplished at the mill prior to cutting the plate material.

Initial plate flatness was also discussed. Since dimensional tolerance will be a key manufacturing challenge, it was agreed that the ASTM A480 flatness tolerance of 9/16 inch was not stringent enough. After discussions with the supplier, it was recommended that the LLL purchase order should specify 1/2 the ASTM tolerance or approximately 1/4 inch.

All final drawings were reviewed by representatives of Thermodynamics, Stress, Design, Materials and Process, Producibility, Quality Assurance and Program Management. A drawing signoff log was maintained for each drawing.

Quality Assurance recommendations for the manufacturing phase of the MFTF magnet system are summarized as follows:

LLL specification for welding and fabrication must be expanded to include more stringent quality assurances of such key items as:

Material Quality - U/S Inspection

Mechanical Property Testing Weldments

Certification of the Welding Process

Certification and Testing of the Welders

LLL-NDE Standards

Dimensional Tolerance Control

The welding of the MFTF magnet must be of the highest quality, free from cracks, voids and other harmful defects. Buying U/S quality plate will help, however since few industrial concerns have had significant experience with welding thick sections of 304LN material, LLL may have to be prepared to demonstrate both the welding and NDE procedures.

The manufacturing sequence and flow for fabrication of the magnet will assist controlling both distortion and dimensional tolerances. These requirements must be rigidly controlled during the subassembly and detail fabrication. Welding sequencing may provide some relief in this regard. The use of tooling templates and optics will be a must in fabricating a structure of this size. Written planning with progressive inspection buy-off will be essential in maintaining subassembly and end item control.